Non-intrusive stochastic analysis with parameterized imprecise probability models: I. performance estimation

Pengfei Wei [a,c*], Jingwen Song[b,c*], Sifeng Bi[c], Matteo Broggi[c], Michael Beer[c,d,e], Zhenzhou Lu[b], Zhufeng Yue[a]

[a] *School of Mechanics, Civil Engineering and Architecture, Northwestern Polytechnical University, Xi'an 710072, China*

[b] *School of Aeronautics, Northwestern Polytechnical University, Xi'an 710072, China*

[c] *Institute for Risk and Reliability, Leibniz Universität Hannover, Callinstr. 34, Hannover, Germany*

[d] *Institute for Risk and Uncertainty, University of Liverpool, Peach Street, L69 7ZF Liverpool, United Kingdom*

[e] *International Joint Research Center for Engineering Reliability and Stochastic Mechanics, Tongji University, Shanghai 200092, China*

Abstract: Uncertainty propagation through the simulation models is critical for computational mechanics engineering to provide robust and reliable design in the presence of polymorphic uncertainty. This set of companion papers present a general framework, termed as *non-intrusive imprecise stochastic simulation*, for uncertainty propagation under the background of imprecise probability. This framework is composed of a set of methods developed for meeting different goals. In this paper, the performance estimation is concerned. The local extended Monte Carlo simulation (EMCS) is firstly reviewed, and then the global EMCS is devised to improve the global performance. Secondly, the cut-HDMR (High-Dimensional Model Representation) is introduced for decomposing the probabilistic response functions, and the local EMCS method is used for estimating the cut-HDMR component functions. Thirdly, the RS (Random Sampling)-HDMR is introduced to decompose the probabilistic response functions, and the global EMCS is applied for estimating the RS-HDMR component functions. The statistical errors of all estimators are derived, and the truncation errors are estimated by two global sensitivity indices, which can also be used for identifying the influential HDMR components. In the companion paper, the reliability and rare event analysis are treated. The effectiveness of the proposed methods are demonstrated by numerical and engineering examples.

Keywords: Imprecise stochastic simulation; Uncertainty quantification; Imprecise probability models; High-dimensional model representation; Sensitivity analysis; Aleatory and epistemic uncertainties

1. Introduction

The rapid development of computational technology has significantly promoted the application of computer-aided design and engineering in the entry life-cycle of productions. However, one of the critical challenge is the presence of the inevitable uncertainties during not only the modelling, but also the manufactural and experimental procedures. The uncertainties can be typically classified into two

* Corresponding author:
pengfeiwei@nwpu.edu.cn (P. Wei) and jwsong0879@163.com (J. Song)
Please cite this paperas: Wei, P., Song, J., Bi, S., Broggi, M., Beer, M., Lu, Z., & Yue, Z. (2019). Non-intrusive stochastic analysis with parameterized imprecise probability models: I. Performance estimation. Mechanical Systems and Signal Processing, 124, 349-368.

categories, i.e., the aleatory uncertainty (natural variation) and the epistemic uncertainty (lack of knowledge) [1][2]. Commonly, the aleatory uncertainty results in occasional failure and/or lack of robustness of engineering structures, while the epistemic uncertainty prevents us from learning the degree of structural reliability and robustness, thus there is a need to distinguish between these two kinds of uncertainties during the whole design process [1]. In practical applications, very often these two kinds of uncertainties are simultaneous in various sources, e.g. parameter imprecision, model approximation, and experiment noise, leading to easily-confused understanding on the effect of these two kinds of uncertainties. Hence, the main objective of this work is to developing a general uncertainty propagation framework based on clearly differentiating the aleatory and epistemic uncertainties, which is critical for uncertainty management during the whole design process of products [3].

During the campaign of uncertainty quantification and propagation, the current methodologies for uncertainty characterization can be classified into three groups, i.e. the non-probabilistic approach, the precise probability approach, and the imprecise probability approach. The non-probabilistic approach includes, for example, the convex model [4], the possibility theory based on fuzzy sets [5], etc. Despite their simple principle and wide applicability, these techniques do not make a distinction between the aleatory and epistemic uncertainties, and in the propagation process, an optimization procedure directly performed on the model response functions is unavoidable [2]. As one of the most mature methodologies for uncertainty characterization, the precise probability approach is applicable for an exclusive kind of uncertainty (epistemic or aleatory) [5][6]. In case for the aleatory uncertainty characterization, generally a large amount of precise data is required for generating a precise probability model. The imprecise probability approach can be seen as a combination of the non-probabilistic approach and the precise probability approach. General techniques of imprecise probability approach include the evidence theory [7], the probability-box (p-box) [8], the fuzzy probability [9], the second-order probability model [10], etc., all of which can be treated in a unified framework [11]. The most attractive feature of the imprecise probability approach is that it characterizes the aleatory and epistemic uncertainties respectively within a double-layer structure, and thus promotes a separation of these two kinds of uncertainties during the propagation process. As it will be shown in this work, another feature of the imprecise probability approach is that the time-consuming optimization performed on the model response functions is no longer obligated during the propagation process. Because of the overall advantages of the imprecise probability approach, this set of companion paper focuses on the uncertainty propagation framework under the imprecise probability background.

Considering the specific field of structural reliability analysis, the imprecise probability propagation approach can be further divided into these three groups: the approximate analytical methods, the surrogate model methods, and the sampling techniques. The approximate analytical methods are initially developed for estimating the structural reliability with precise probability models, and the general techniques include the first-order reliability method (FORM) [12], the second-order reliability method (SORM) [13], and the moment-based method [14]. Both FORM and SORM have been extended to estimate the failure probability bounds with input variables characterized using the evidence theory by expending the limit state function at the so-called “most-probable focal element” with Taylor series [15]. The moment-based method has be utilized in reliability analysis with input variables characterized using

parameterized p-box model by estimating the bounds of response moments and approximating the probability density function (PDF) of response with Johnson types of distributions [16]. The estimation errors of this group of methods come from two aspects, i.e., the approximation errors for computing response moments and the difference between the true response distributions and the assumed ones, both of which are difficult to assess.

In the precise probability framework, the surrogate model approach combined or not combined with the active learning has been widely used for uncertainty propagation and reliability analysis [17][18]. Recently, this method has been extended to imprecise probability approaches. In Ref. [19], a two-level surrogate model procedure was proposed for propagating p-box models based on non-intrusive sparse polynomial chaos expansions. And this procedure was later extended to estimate the bound of failure probability by combining Kriging surrogate model with active learning procedure [20]. A one-level surrogate model method based on Kriging model and active learning procedure was proposed for estimating the failure probability bounds with input variables characterized by evidence theory [21]. However, these surrogate models are commonly not applicable to high-dimensional (typically higher than 20-dimensional) problems.

A series of advanced sampling techniques have been developed for precise probability applications, such as importance sampling [22], line sampling [23], subset simulation [24], and directional sampling [25]. The subset simulation has also been extended for estimating the bounds of small failure probability with input variables characterized by any imprecise probability models [11]. Two specific sampling techniques, denoted as Interval Monte Carlo simulation (IMCS) [26] and Extended Monte Carlo simulation (EMCS) [27], have been developed for propagating the imprecise probability models. The IMCS is an intrusive procedure which requires interval finite element analysis for each interval sample, while the EMCS developed in the authors' previous work [27] is a non-intrusive procedure applicable to any black-box models. Compared with the IMCS method, the EMCS method is demonstrated to possess a wider application range, since it has been applied to global sensitivity analysis where the input variables are described under the imprecise probability sense [28]. This method was also later reported in Ref. [29] with emphasis on specifying the sampling density. However, a disadvantage of the EMCS method is that, the variances of the unbiased EMCS estimators tend to be extremely large for problems with numerous epistemic parameters [27].

This set of companion papers aim at developing a new general framework, called *non-intrusive imprecise stochastic simulation*, for efficiently and accurately propagating the parameterized imprecise probability models through any black computational model. This paper concentrates on general performance estimation, while the companion paper focuses on the reliability and rare failure event analysis. To achieve this objective, the so-called Global EMCS (GEMCS) is proposed to extend the classical EMCS, such that a better performance in the uncertain parameter space can be achieved. For clarity, the classical EMCS is termed as Local EMCS (LEMCS) in the following context. Then, the cut high-dimensional model representation (cut-HDMR) method is utilized to improve the LEMCS procedure, and the Random Sampling (RS-) HDMR method is utilized to improve the GEMCS procedure. Different with the HDMR methods used for approximating the model response functions, the HDMR methods in this work do not require any surrogate model, thus the estimation errors are easier to assess

based purely on the statistical properties the EMCS estimators. The global sensitivity analysis techniques are also utilized in this work to quantify the truncation errors of the HDMR models, and furthermore to measure the relative importance of the HDMR components.

The rest of this paper is organized as follows. Section 2 reviews the classical LEMCS method, and subsequently proposes the novel GEMCS method. In Section 3, the cut-HDMR decomposition method is developed to improve the LEMCS procedure. The GEMCS procedure is further improved by the proposed RS-HDMR decomposition method in Section 4. The feasibility and efficiency of the overall imprecise stochastic simulation framework is demonstrated by both numerical and engineering examples in Section 5. Section 6 presents discussions and key conclusions of this work.

2. Extended Monte Carlo simulation procedures

The EMCS method was originally proposed in Ref. [27] to efficiently estimate the probabilistic response functions (e.g., the first- and second- order origin moment functions) w.r.t. the distribution parameters of the input variables based on the idea of importance sampling. In the classical EMCS method, the unbiased estimators are derived based on the sample points generated by establishing sampling PDFs of input variables with distribution parameters being fixed at a specific point, thus it is termed as LEMCS. In this section, we firstly review this classical procedure, and propose the further improved GEMCS where no fixed point of distribution parameter is required.

Let $y = g(\boldsymbol{x})$ indicate the model response function (also called *g*-function for simplicity), where $\boldsymbol{x} = (x_1, x_2, \ldots, x_n)^T$ is the *n*-dimensional input variables, and y is the model output of interest. In reliability analysis, the structure failure is denoted by the situation when y is less than zero. Hence, the failure domain is defined as $F = \{\boldsymbol{x} : g(\boldsymbol{x}) < 0\}$, and the indicator function of the failure domain is expressed as $I_F(\boldsymbol{x}) = 1$ if $\boldsymbol{x} \in F$, and $I_F(\boldsymbol{x}) = 0$ if $\boldsymbol{x} \notin F$.

In this work, we only consider the parameterized imprecise probability models. Under probabilistic representation, the joint PDF of $\boldsymbol{x}$ is denoted as $f_X(\boldsymbol{x}|\boldsymbol{\theta})$, where $\boldsymbol{\theta} = (\theta_1, \theta_2, \ldots, \theta_d)^T$ is the *d*-dimensional vector of distribution parameters. Because of the epistemic uncertainty, the distribution parameters are not fully determined, but also uncertain. For example, for *p*-box model, the epistemic uncertainty of $\boldsymbol{\theta}$ is characterized by intervals or general convex model [8]; for fuzzy probability model, $\boldsymbol{\theta}$ is described by fuzzy set model [9]; for second-order probability model, $\boldsymbol{\theta}$ is represented by subjective probability model [10]. The joint PDF of $\boldsymbol{\theta}$ is assumed to be $f_{\boldsymbol{\Theta}}(\boldsymbol{\theta})$. In this work, we assume that $\boldsymbol{\theta}$ are independent, i.e., $f_{\boldsymbol{\Theta}}(\boldsymbol{\theta}) = \prod_{i=1}^{d} f_{\Theta_i}(\theta_i)$, where $f_{\Theta_i}(\theta_i)$ indicates the marginal PDF of θ_i. We refer to $f_X(\boldsymbol{x}|\boldsymbol{\theta})$ as the conditional joint PDF of $\boldsymbol{x}$ conditional on $\boldsymbol{\theta}$, and $f_{X,\boldsymbol{\Theta}}(\boldsymbol{x}, \boldsymbol{\theta}) = f_X(\boldsymbol{x}|\boldsymbol{\theta}) f_{\boldsymbol{\Theta}}(\boldsymbol{\theta})$ as the joint PDF of $\boldsymbol{x}$ and $\boldsymbol{\theta}$.

Note that, among all the imprecise probability models, only a small fraction (e.g., the second-order probability model) attributes subjective probability distributions to $\boldsymbol{\theta}$. Introducing probability distributions for $\boldsymbol{\theta}$ is just an instrumental tool for performing the proposed methods, but doesn't imply that the proposed methods are only restricted to the second-order probability model. In fact, the proposed

methods can be applied to any parameterized imprecise probability models.

Let $\mathrm{E}_y(\boldsymbol{\theta})$, $\mathrm{V}_y(\boldsymbol{\theta})$ and $\mathrm{P}_f(\boldsymbol{\theta})$ indicate the first- and second- order origin moment functions as well as the failure probability function, respectively, which can be expressed as:

$$\begin{cases} \mathrm{E}_y(\boldsymbol{\theta}) = \int g(\boldsymbol{x}) f_X(\boldsymbol{x}\,|\,\boldsymbol{\theta}) \mathrm{d}\boldsymbol{x} \\ \mathrm{V}_y(\boldsymbol{\theta}) = \int g^2(\boldsymbol{x}) f_X(\boldsymbol{x}\,|\,\boldsymbol{\theta}) \mathrm{d}\boldsymbol{x} \\ \mathrm{P}_f(\boldsymbol{\theta}) = \int I_F(\boldsymbol{x}) f_X(\boldsymbol{x}\,|\,\boldsymbol{\theta}) \mathrm{d}\boldsymbol{x} \end{cases}. \tag{1}$$

The basic idea behind LEMCS procedure for estimating the above three functions adapts from the importance sampling. Firstly, a fixed point $\boldsymbol{\theta}^*$ should be assigned $\boldsymbol{\theta}$ such that to obtain a sampling PDF $f_X(\boldsymbol{x}\,|\,\boldsymbol{\theta}^*)$ for the input variables. Then the LEMCS estimators of the three functions in Eq.(1) was derived as [27]:

$$\begin{cases} \hat{\mathrm{E}}_y(\boldsymbol{\theta}) = \dfrac{1}{N}\sum_{k=1}^{N} g\left(\boldsymbol{x}^{(k)}\right) \dfrac{f_X\left(\boldsymbol{x}^{(k)}\,|\,\boldsymbol{\theta}\right)}{f_X\left(\boldsymbol{x}^{(k)}\,|\,\boldsymbol{\theta}^*\right)} \\ \hat{\mathrm{V}}_y(\boldsymbol{\theta}) = \dfrac{1}{N}\sum_{k=1}^{N} g^2\left(\boldsymbol{x}^{(k)}\right) \dfrac{f_X\left(\boldsymbol{x}^{(k)}\,|\,\boldsymbol{\theta}\right)}{f_X\left(\boldsymbol{x}^{(k)}\,|\,\boldsymbol{\theta}^*\right)} \\ \hat{\mathrm{P}}_f(\boldsymbol{\theta}) = \dfrac{1}{N}\sum_{k=1}^{N} I_F\left(\boldsymbol{x}^{(k)}\right) \dfrac{f_X\left(\boldsymbol{x}^{(k)}\,|\,\boldsymbol{\theta}\right)}{f_X\left(\boldsymbol{x}^{(k)}\,|\,\boldsymbol{\theta}^*\right)} \end{cases} \tag{2}$$

where $\boldsymbol{x}^{(k)}$ ($k = 1, 2, \ldots, N$) indicates the N sample points generated from $f_X(\boldsymbol{x}\,|\,\boldsymbol{\theta}^*)$. The above estimators are unbiased by nature, and their performances are highly affected by the fixed point $\boldsymbol{\theta}^*$. In Ref. [27], a technique was proposed to appoint a suitable $\boldsymbol{\theta}^*$ allowing $f_X(\boldsymbol{x}\,|\,\boldsymbol{\theta}^*)$ and $f_X(\boldsymbol{x}\,|\,\boldsymbol{\theta})$ have the same support domains. In fact, the LEMCS estimators often perform well in the region around $\boldsymbol{\theta}^*$, thus $\boldsymbol{\theta}^*$ should be specified to be the point around which the values of the probabilistic response functions are of interest. In this work, we just assume that $\boldsymbol{\theta}^*$ is fixed at the mean point of $\boldsymbol{\theta}$.

The LEMCS procedure performs well around the local points $\boldsymbol{\theta}^*$, but large estimation errors may present at the points far from $\boldsymbol{\theta}^*$ due to the large diversity of the realizations of the ratio $f_X(\boldsymbol{x}\,|\,\boldsymbol{\theta}) / f_X(\boldsymbol{x}\,|\,\boldsymbol{\theta}^*)$. To improve the global performance of the LEMCS procedure, we propose the GEMCS procedure. The GEMCS estimators are derived based on a joint sample set $\left(\boldsymbol{x}^{(k)}, \boldsymbol{\theta}^{(k)}\right)$ ($k = 1, 2, \ldots, N$) generated from the joint PDF $f_{X,\boldsymbol{\Theta}}(\boldsymbol{x}, \boldsymbol{\theta})$. Take the Latin Hypercube Sampling (LHS) technique as an example, the procedure for generating the joint sample sets are presented as follows.

Step 1: Generate a sample matrix $\mathbf{U} = \left(u_{kl}\right)_{k=1,2,\ldots N, l=1,2,\ldots,n+d}$ of dimension $(N, n+d)$ with each column following independent uniform distribution between 0 and 1.

Step 2: Generate $\boldsymbol{\theta}^{(k)}$ by performing the inverse probability integration transformation (PIT) $\boldsymbol{\theta}^{(k)} = F_{\boldsymbol{\Theta}}^{-1}\left(\boldsymbol{u}_{(n+1:d)}^{(k)}\right)$, where $F_{\boldsymbol{\Theta}}^{-1}(\bullet)$ indicates the inverse cumulative distribution function (CDF) of $\boldsymbol{\theta}$,

and $\boldsymbol{u}_{(n+1:n+d)}^{(k)}$ implies the vector of the k-th row of the sample matrix $\mathbf{U}$ taken from the n+1 to n+d columns.

Step 3: Generate $\boldsymbol{x}^{(k)}$ by performing the inverse PIT $\boldsymbol{x}^{(k)} = F_{\boldsymbol{X}}^{-1}\left(\boldsymbol{u}_{(1:n)}^{(k)} \mid \boldsymbol{\theta}^{(k)}\right)$, where $F_{\boldsymbol{X}}^{-1}\left(\bullet \mid \boldsymbol{\theta}^{(k)}\right)$ refers to the inverse CDF of $\boldsymbol{x}$ conditional on $\boldsymbol{\theta}$=$\boldsymbol{\theta}^{(k)}$, and $\boldsymbol{u}_{(1:n)}^{(k)}$ indicates the n-dimensional vector taken from the k-th row and columns from 1 to n of the sample matrix $\mathbf{U}$.

Then, based on the generated joint sample set, the unbiased GEMCS estimators for $\mathrm{E}_y(\boldsymbol{\theta})$, $\mathrm{V}_y(\boldsymbol{\theta})$ and $\mathrm{P}_f(\boldsymbol{\theta})$ are derived as:

$$\begin{cases} \hat{\mathrm{E}}_y(\boldsymbol{\theta}) = \dfrac{1}{N}\sum_{k=1}^{N} g\left(\boldsymbol{x}^{(k)}\right) \dfrac{f_{\boldsymbol{X}}\left(\boldsymbol{x}^{(k)} \mid \boldsymbol{\theta}\right)}{f_{\boldsymbol{X}}\left(\boldsymbol{x}^{(k)} \mid \boldsymbol{\theta}^{(k)}\right)} \\ \hat{\mathrm{V}}_y(\boldsymbol{\theta}) = \dfrac{1}{N}\sum_{k=1}^{N} g^2\left(\boldsymbol{x}^{(k)}\right) \dfrac{f_{\boldsymbol{X}}\left(\boldsymbol{x}^{(k)} \mid \boldsymbol{\theta}\right)}{f_{\boldsymbol{X}}\left(\boldsymbol{x}^{(k)} \mid \boldsymbol{\theta}^{(k)}\right)} \\ \hat{\mathrm{P}}_f(\boldsymbol{\theta}) = \dfrac{1}{N}\sum_{k=1}^{N} I_F\left(\boldsymbol{x}^{(k)}\right) \dfrac{f_{\boldsymbol{X}}\left(\boldsymbol{x}^{(k)} \mid \boldsymbol{\theta}\right)}{f_{\boldsymbol{X}}\left(\boldsymbol{x}^{(k)} \mid \boldsymbol{\theta}^{(k)}\right)} \end{cases}. \tag{3}$$

The proof of the above GEMCS estimators is reported in Appendix A. In Eq.(3), the sample points of $\boldsymbol{\theta}$ spread over their full supports, thus these estimators perform better than those in Eq.(2) in a global sense, but they may be less accurate than those in Eq. (2) at the points around $\boldsymbol{\theta}^*$.

The above LEMCS and GEMCS procedures can also be extended to estimate the central moment functions (e.g., responses variance function), Sobol's variance-based sensitivity functions [28][30], the response PDF function, etc., w.r.t. the input distribution parameters. In this part, we take the origin moment functions and the failure probability functions as examples to illustrate the proposed methods. For the failure probability function, the estimators in Eqs. (2) and (3) can also be used, but they are only applicable for structures with relatively large failure probabilities. For rare failure events, these estimators are computationally too expensive. In the companion paper, we propose comprehensive improvements for the estimation of the failure probability function subjected to rare failure events.

Despite the improvement of the global performance, the standard deviations (SDs) of the estimators in Eqs. (2) and (3) tend to increase w.r.t. the dimension of $\boldsymbol{\theta}$, and commonly, these two methods do not perform well in high dimension. The essential reason is that, in the high-dimensional situations, the samples of the ratio $f_{\boldsymbol{X}}(\boldsymbol{x} \mid \boldsymbol{\theta}) \big/ f_{\boldsymbol{X}}(\boldsymbol{x} \mid \boldsymbol{\theta}^*)$ in Eq. (2) and the ratio $f_{\boldsymbol{X}}\left(\boldsymbol{x}^{(k)} \mid \boldsymbol{\theta}\right) \big/ f_{\boldsymbol{X}}\left(\boldsymbol{x}^{(k)} \mid \boldsymbol{\theta}^{(k)}\right)$ in Eq.(3) tend to have larger variations than those in the low-dimensional situations, which inversely, result in large variances of the estimators in Eqs. (2) and (3). This phenomenon makes both the LEMCS and GEMCS procedures not applicable in most real applications. To deal this disadvantage, we firstly introduce the cut-HDMR to improve the LEMCS procedure in the next section.

3. Combination of LEMCS with cut-HDMR

The HDMR method is an effective function decomposition method, and it has been widely used for developing surrogate models and sensitivity analysis techniques [31]-[33]. There are generally two kinds of HDMR models, i.e., the cut-HDMR [34] and the RS-HDMR [35]. In this section, the cut-HDMR is

introduced to improve the performance of the LEMCS estimators in high dimension.

Take the response expectation function $\mathrm{E}_y(\boldsymbol{\theta})$ as an example, both the cut-HDMR and RS-HDMR decompositions are formulated as:

$$\mathrm{E}_y(\boldsymbol{\theta}) = \mathrm{E}_{y0} + \sum_{i=1}^{d} \mathrm{E}_{yi}(\theta_i) + \sum_{1\le i<j\le d} \mathrm{E}_{yij}(\boldsymbol{\theta}_{ij}) + \ldots + \mathrm{E}_{y12\ldots d}(\boldsymbol{\theta}) \tag{4}$$

where $\boldsymbol{\theta}_{ij}$ indicates the 2-dimensional vector consists of θ_i and θ_j. For the cut-HDMR decomposition, the component functions in Eq.(4) possess the following forms:

$$\mathrm{E}_{\mathrm{cut}\,y0} = \mathrm{E}_y(\boldsymbol{\theta}^*) = \int g(\boldsymbol{x})\, f_X(\boldsymbol{x}\,|\,\boldsymbol{\theta}^*)\,\mathrm{d}\boldsymbol{x} \tag{5}$$

$$\mathrm{E}_{\mathrm{cut}\,yi}(\theta_i) = \mathrm{E}_y(\theta_i, \boldsymbol{\theta}^*_{-i}) - \mathrm{E}_{\mathrm{cut}\,y0} = \int g(\boldsymbol{x})\, f_X(\boldsymbol{x}\,|\,\theta_i, \boldsymbol{\theta}^*_{-i})\,\mathrm{d}\boldsymbol{x} - \mathrm{E}_{\mathrm{cut}\,y0} \tag{6}$$

$$\begin{aligned} \mathrm{E}_{\mathrm{cut}\,yij}(\boldsymbol{\theta}_{ij}) &= \mathrm{E}_y(\boldsymbol{\theta}_{ij}, \boldsymbol{\theta}^*_{-ij}) - \mathrm{E}_{\mathrm{cut}\,yi}(\theta_i) - \mathrm{E}_{\mathrm{cut}\,yj}(\theta_j) - \mathrm{E}_{\mathrm{cut}\,y0} \\ &= \int g(\boldsymbol{x})\, f_X(\boldsymbol{x}\,|\,\boldsymbol{\theta}_{ij}, \boldsymbol{\theta}^*_{-ij})\,\mathrm{d}\boldsymbol{x} - \mathrm{E}_{\mathrm{cut}\,yi}(\theta_i) - \mathrm{E}_{\mathrm{cut}\,yj}(\theta_j) - \mathrm{E}_{\mathrm{cut}\,y0} \end{aligned} \tag{7}$$

…

where the word 'cut' in the subscript of each component function indicates that they are the cut-HDMR component functions instead of the RS-HDMR ones, $\boldsymbol{\theta}_{-i}$ refers to the (d-1)-dimensional vector including all the distribution parameters but θ_i, and $\boldsymbol{\theta}^*$ is a fixed point, which can be simply set as the same as that of the LEMCS method.

All the cut-HDMR component functions possess the vanishing property, which means that, when any distribution parameter θ_{i_a} involved in the component function $\mathrm{E}_{\mathrm{cut}\,yi_1i_2\ldots,i_s}(\boldsymbol{\theta}_{i_1i_2\ldots i_s})$ is fixed at the expansion point $\theta^*_{i_a}$, this component function equals to zero [34], i.e.,

$$\mathrm{E}_{\mathrm{cut}\,yi_1i_2\ldots,i_s}(\boldsymbol{\theta}_{i_1i_2\ldots i_s})\Big|_{\theta_{i_a}=\theta^*_{i_a}} = 0, \qquad i_a \in \{i_1, i_2, \ldots, i_s\} \subseteq \{1, 2, \ldots, d\}. \tag{8}$$

The vanishing property indicates that each cut-HDMR component function equals to zero at any base lines or base planes $\theta_{i_a} = \theta^*_{i_a}$. The cut-HDMR component functions also satisfy the property of mutual orthogonality, which indicates that, when any distribution parameter θ_{i_s}, belonging to the union set of the distribution parameters involved in two component functions $\mathrm{E}_{\mathrm{cut}\,yi_1i_2\ldots,i_s}(\boldsymbol{\theta}_{i_1i_2\ldots i_s})$ and $\mathrm{E}_{\mathrm{cut}\,yj_1j_2\ldots,j_t}(\boldsymbol{\theta}_{j_1j_2\ldots j_t})$, is fixed at $\theta^*_{i_a}$, the product of these two component functions equals to zero [34], i.e.,

$$\mathrm{E}_{\mathrm{cut}\,yi_1i_2\ldots,i_s}(\boldsymbol{\theta}_{i_1i_2\ldots i_s})\,\mathrm{E}_{\mathrm{cut}\,yj_1j_2\ldots,j_t}(\boldsymbol{\theta}_{j_1j_2\ldots j_t})\Big|_{\theta_{i_a}=\theta^*_{i_a}} = 0, \qquad i_a \in \{i_1, i_2, \ldots, i_s\} \cup \{j_1, j_2, \ldots, j_t\}. \tag{9}$$

The above two properties will also be demonstrated by the results of the test examples in Section 5.

The cut-HDMR decomposition can be interpreted based on Taylor series expansion [34]. As it has been well-known, the Taylor series expansion consists of infinite number of component functions. The constant term in Eq.(5) is the same as the constant term of Taylor series expansion; the univariate component function $\mathrm{E}_{\mathrm{cut}\,yi}(\theta_i)$ in Eq. (6) consists of all the Taylor series terms containing only θ_i; the bivariate component function $\mathrm{E}_{\mathrm{cut}\,yij}(\boldsymbol{\theta}_{ij})$ in Eq. (7) is the summation of all the Taylor series terms

contain only x_i and x_j; higher order component functions in Eq.(4) can be similarly interpreted. Thus, the low-order component functions in Eq. (4) provide a perfect approximation to the nonlinearity and low-order interactions of the response expectation function $\mathrm{E}_y(\boldsymbol{\theta})$. It has been demonstrated by many researchers, very often the second-order HDMR approximations provide satisfactory results [34][35]. Thus, for approximating the probabilistic response functions, commonly only the first- and second- order cut-HDMR component functions need to be estimated. Thus, the combination of LEMCS with cut-HDMR can provide better estimation for any probabilistic response functions, and we denote this method as "LEMCS-cut-HDMR".

Based on the sample points $\boldsymbol{x}^{(k)}$ ($k=1,2,\ldots,N$) generated from $f_X(\boldsymbol{x}\,|\,\boldsymbol{\theta}^*)$ and the corresponding response values $y^{(k)}=g(\boldsymbol{x}^{(k)})$, the estimators of the cut-HDMR component functions in Eqs. (5)-(7) can be derived as:

$$\begin{cases} \hat{\mathrm{E}}_{\mathrm{cut}\,y0}(\boldsymbol{\theta}^*)=\dfrac{1}{N}\displaystyle\sum_{j=1}^{N}y^{(k)} \\ \hat{\mathrm{E}}_{\mathrm{cut}\,yi}(\theta_i)=\dfrac{1}{N}\displaystyle\sum_{k=1}^{N}y^{(k)}r_{\mathrm{cut}\,i}(\boldsymbol{x}^{(k)}\,|\,\theta_i,\boldsymbol{\theta}^*) \\ \hat{\mathrm{E}}_{\mathrm{cut}\,yij}(\boldsymbol{\theta}_{ij})=\dfrac{1}{N}\displaystyle\sum_{k=1}^{N}y^{(k)}r_{\mathrm{cut}\,ij}(\boldsymbol{x}^{(k)}\,|\,\boldsymbol{\theta}_{ij},\boldsymbol{\theta}^*) \end{cases} \tag{10}$$

where

$$\begin{cases} r_{\mathrm{cut}\,i}(\boldsymbol{x}^{(k)}\,|\,\theta_i,\boldsymbol{\theta}^*)=\dfrac{f_{\mathrm{X}}(\boldsymbol{x}^{(k)}\,|\,\theta_i,\boldsymbol{\theta}^*_{-i})}{f_{\mathrm{X}}(\boldsymbol{x}^{(k)}\,|\,\boldsymbol{\theta}^*)}-1 \\ r_{\mathrm{cut}\,ij}(\boldsymbol{x}^{(k)}\,|\,\boldsymbol{\theta}_{ij},\boldsymbol{\theta}^*)=\dfrac{f_{\mathrm{X}}(\boldsymbol{x}^{(k)}|\boldsymbol{\theta}_{ij},\boldsymbol{\theta}^*_{-ij})}{f_{\mathrm{X}}(\boldsymbol{x}^{(k)}|\boldsymbol{\theta}^*)}-\dfrac{f_{\mathrm{X}}(\boldsymbol{x}^{(k)}|\theta_i,\boldsymbol{\theta}^*_{-i})}{f_{\mathrm{X}}(\boldsymbol{x}^{(k)}|\boldsymbol{\theta}^*)}-\dfrac{f_{\mathrm{X}}(\boldsymbol{x}^{(k)}|\theta_j,\boldsymbol{\theta}^*_{-j})}{f_{\mathrm{X}}(\boldsymbol{x}^{(k)}|\boldsymbol{\theta}^*)}+1 \end{cases}. \tag{11}$$

The estimators in Eq.(10) are unquestionably unbiased, and their variances can be computed by:

$$\begin{cases} \mathrm{var}(\hat{\mathrm{E}}_{\mathrm{cut}\,y0})\doteq\dfrac{1}{N(N-1)}\left[\displaystyle\sum_{k=1}^{N}y^{(k)2}-N\hat{\mathrm{E}}^2_{\mathrm{cut}\,y0}\right] \\ \mathrm{var}(\hat{\mathrm{E}}_{\mathrm{cut}\,yi})\doteq\dfrac{1}{N(N-1)}\left\{\displaystyle\sum_{k=1}^{N}y^{(k)2}r^2_{\mathrm{cut}\,i}(\boldsymbol{x}^{(k)}\,|\,\theta_i,\boldsymbol{\theta}^*)-N\hat{\mathrm{E}}^2_{\mathrm{cut}\,yi}\right\} \\ \mathrm{var}(\hat{\mathrm{E}}_{\mathrm{cut}\,yij})\doteq\dfrac{1}{N(N-1)}\left\{\displaystyle\sum_{k=1}^{N}y^{(k)2}r^2_{\mathrm{cut}\,ij}(\boldsymbol{x}^{(k)}\,|\,\boldsymbol{\theta}_{ij},\boldsymbol{\theta}^*)-N\hat{\mathrm{E}}^2_{\mathrm{cut}\,yij}\right\} \end{cases}. \tag{12}$$

One can refer to Appendix B for derivations of Eqs. (10)-(12). Then, as the estimators in Eq.(10) approximately follow normal distribution, their confidence intervals can be derived. For example, $\left[\hat{\mathrm{E}}_{\mathrm{cut}\,y0}-2\sqrt{\mathrm{var}(\hat{\mathrm{E}}_{\mathrm{cut}\,y0})},\hat{\mathrm{E}}_{\mathrm{cut}\,y0}+2\sqrt{\mathrm{var}(\hat{\mathrm{E}}_{\mathrm{cut}\,y0})}\right]$ indicates the 95.45% confidence interval of $\mathrm{E}_{\mathrm{cuty0}}$.

The estimators in Eq. (10) indicate that the first- and second- order component functions of the response moment functions can be estimated with only one set of samples generated from $f_X(\boldsymbol{x}\,|\,\boldsymbol{\theta}^*)$, and the computational cost does not increase w.r.t. the dimension of $\boldsymbol{\theta}$. We can also derive the LEMCS estimators for higher order cut-HDMR component functions if necessary, and this will not increase the

computational cost obviously. The above procedure can be easily extended to the second-order origin moment function $\mathrm{V}_y(\boldsymbol{\theta})$ and the failure probability function $\mathrm{P}_f(\boldsymbol{\theta})$, which is not repeated for clarity.

It is easy to prove that the estimators in Eq. (10) also possess the vanishing property and mutually orthogonal property. Take the estimators $\hat{\mathrm{E}}_{\mathrm{cut}\,yij}$ in Eq.(10) as an example. If any one of θ_i and θ_j is fixed at its expansion point, then one can verify that the ratio $r_{\mathrm{cut}\,ij}\left(\boldsymbol{x}^{(j)} \mid \boldsymbol{\theta}_{ij}, \boldsymbol{\theta}^*\right)$ equals to zero, resulting in the identically vanishing of $\hat{\mathrm{E}}_{\mathrm{cut}\,yij}$. For estimators $\hat{\mathrm{E}}_{\mathrm{cut}\,yi}$ and $\hat{\mathrm{E}}_{\mathrm{cut}\,yij}$ in Eq.(10), if their common distribution parameter θ_i is fixed at the expansion point θ_i^*, then the ratio functions involved in both estimators equal to zero constantly, resulting in the mutual orthogonality of these estimators. The above conclusions can be extended to the estimators of any higher order component functions.

Based on the vanishing property, we can judge whether a component function is influential or not based on the average distance from its realizations to the origin line or origin plane. The larger the average distance is, the more influential this component function is. But this is just a qualitative judgement. For quantitatively judging the relative importance of each component function, we introduce the following sensitivity index:

$$S_{\mathrm{Ecut}\,i_1 i_2 \ldots i_s} = \frac{\mathrm{var}_{\boldsymbol{\Theta}_{i_1 i_2 \ldots i_s}}\left[\mathrm{E}_{\mathrm{cut}\,i_1 i_2 \ldots i_s}\left(\boldsymbol{\theta}_{i_1 i_2 \ldots i_s}\right)\right]}{\sum\limits_{\{i_1, i_2, \ldots, i_t\} \subset \{1,2,\ldots,d\}} \mathrm{var}_{\boldsymbol{\Theta}_{i_1 i_2 \ldots i_t}}\left[\mathrm{E}_{\mathrm{cut}\,i_1 i_2 \ldots i_t}\left(\boldsymbol{\theta}_{i_1 i_2 \ldots i_t}\right)\right]} \quad \left|\{i_1, i_2, \ldots, i_s\}\right| \le M \tag{13}$$

where $\mathrm{var}_{\boldsymbol{\Theta}_{i_1 i_2 \ldots i_s}}[\bullet]$ refers to the variance operator w.r.t. $\boldsymbol{\theta}_{i_1 i_2 \ldots i_s}$, $|\bullet|$ indicates the total number of elements contained in the set, M refers to the maximum order under consideration. By definition, $S_{\mathrm{Ecut}\,i_1 i_2 \ldots i_s}$ is bounded between 0 and 1, and the larger this value is, the more influential the corresponding component function is. The sensitivity index $S_{\mathrm{Ecut}\,i_1 i_2 \ldots i_s}$ can be estimated by numerical integration techniques as commonly only one or two dimensional integrals need to be computed.

As it will be demonstrated in the example section, this method has desirable local performance around the fixed point $\boldsymbol{\theta}^*$. This is due to the fact that, at the points near by $\boldsymbol{\theta}^*$, the scatter degrees of the sample values of the ratios in Eq. (11) are commonly very small, resulting in small variances of the estimators in Eq.(10). In some applications, the values of $\boldsymbol{\theta}$ of interest may be very far from the fixed point $\boldsymbol{\theta}^*$, which may result in large estimation errors of the component functions at these points. In this situation, we can perform a multi-points based LEMCS-cut-HDMR procedure which involves specifying multiple expansion points for cut-HDMR. This multi-points based method is fairly effective due to the excellent local performance of the LEMCS-cut-HDMR procedure. In the next section, we propose a new method by combining the GEMCS method and RS-HDMR method.

4. Combination of GEMCS with RS-HDMR

The RS-HDMR decomposition also takes the form of Eq.(4), but the component functions are differently formulated with those of the cut-HDMR decomposition. Take the response expectation function $\mathrm{E}_y(\boldsymbol{\theta})$ as an example, the RS-HDMR component functions are expressed as follow [35]:

$$\mathrm{E}_{\mathrm{RS}\,y0} = \mathrm{Exp}_{\boldsymbol{\Theta}}\left[\mathrm{E}_y(\boldsymbol{\theta})\right] = \int g(\boldsymbol{x})\, f_X(\boldsymbol{x} \mid \boldsymbol{\theta})\, f_{\boldsymbol{\Theta}}(\boldsymbol{\theta})\, \mathrm{d}\boldsymbol{x}\mathrm{d}\boldsymbol{\theta} \tag{14}$$

$$\mathrm{E}_{\mathrm{RS}yi}\left(\theta_i\right)=\mathrm{Exp}_{\boldsymbol{\Theta}_{-i}}\left[\mathrm{E}_y\left(\boldsymbol{\theta}\right)|\,\theta_i\right]-\mathrm{E}_{\mathrm{RS}y0}=\int g\left(\boldsymbol{x}\right)f_X\left(\boldsymbol{x}\,|\,\boldsymbol{\theta}\right)f_{\boldsymbol{\Theta}_{-i}}\left(\boldsymbol{\theta}_{-i}\right)\mathrm{d}\boldsymbol{x}\mathrm{d}\boldsymbol{\theta}_{-i}-\mathrm{E}_{\mathrm{RS}y0} \tag{15}$$

$$\begin{aligned}\mathrm{E}_{\mathrm{RS}yij}\left(\boldsymbol{\theta}_{ij}\right)&=\mathrm{Exp}_{\boldsymbol{\Theta}_{-ij}}\left[\mathrm{E}_y\left(\boldsymbol{\theta}\right)|\,\boldsymbol{\theta}_{ij}\right]-\mathrm{E}_{\mathrm{RS}yi}\left(\theta_i\right)-\mathrm{E}_{\mathrm{RS}yj}\left(\theta_j\right)-\mathrm{E}_{\mathrm{RS}y0}\\&=\int g\left(\boldsymbol{x}\right)f_X\left(\boldsymbol{x}\,|\,\boldsymbol{\theta}\right)f_{\boldsymbol{\Theta}_{-ij}}\left(\boldsymbol{\theta}_{-ij}\right)\mathrm{d}\boldsymbol{x}\mathrm{d}\boldsymbol{\theta}_{-ij}-\mathrm{E}_{\mathrm{RS}yi}\left(\theta_i\right)-\mathrm{E}_{\mathrm{RS}yj}\left(\theta_j\right)-\mathrm{E}_{\mathrm{RS}y0}\end{aligned} \tag{16}$$

…

where $\mathrm{Exp}_{\boldsymbol{\Theta}}\left[\bullet\right]$ indicates the expectation operator w.r.t $\boldsymbol{\theta}$, $\mathrm{Exp}_{\boldsymbol{\Theta}_{-i}}\left[\bullet\,|\,\theta_i\right]$ is the conditional expectation operator w.r.t. $\boldsymbol{\theta}_{-i}$ conditional on θ_i.

The RS-HDMR component functions also possess two important properties. The first one is the vanishing property, implying that the expectation of each component function equals to zero, i.e.,

$$\mathrm{Exp}_{\{i_1i_2\ldots i_s\}}\left[\mathrm{E}_{\mathrm{RS}yi_1i_2\ldots i_s}\left(\boldsymbol{\theta}_{i_1i_2\ldots i_s}\right)\right]=0\qquad\forall\left\{i_1,i_2,\ldots,i_s\right\}\subseteq\left\{1,2,\ldots,d\right\}. \tag{17}$$

The second property is the mutual orthogonality, implying that the covariance between each pair of component functions equals to zero, i.e.,

$$\begin{aligned}&\mathrm{Exp}_{\{i_1,i_2,\ldots,i_s\}\cup\{j_1,j_2,\ldots,j_t\}}\left[\mathrm{E}_{\mathrm{RS}yi_1i_2\ldots i_s}\left(\boldsymbol{\theta}_{i_1i_2\ldots i_s}\right)\mathrm{E}_{\mathrm{RS}yj_1j_2\ldots j_t}\left(\boldsymbol{\theta}_{j_1j_2\ldots j_t}\right)\right]=0,\\&\forall\left\{i_1,i_2,\ldots,i_s\right\},\left\{j_1,j_2,\ldots,j_t\right\}\subseteq\left\{1,2,\ldots,d\right\}\ \text{ and }\ \left\{i_1,i_2,\ldots,i_s\right\}\neq\left\{j_1,j_2,\ldots,j_t\right\}.\end{aligned} \tag{18}$$

This property holds when the distribution parameters are independent and the response expectation function is square-integrable. This property provides an elegant way for analyzing the truncation error of the RS-HDMR decomposition based on Sobol' sensitivity indices, which is demonstrated later in this section.

Based on the joint sample $\left(\boldsymbol{x}^{(k)},\boldsymbol{\theta}^{(k)}\right)$ ($k=1,2,\ldots,N$) generated from $f_{\boldsymbol{X},\boldsymbol{\Theta}}\left(\boldsymbol{x},\boldsymbol{\theta}\right)$, and the corresponding response values $y^{(k)}=g\left(\boldsymbol{x}^{(k)}\right)$, the unbiased GEMCS estimators of the RS-HDMR component functions can be derived as:

$$\begin{cases}\hat{\mathrm{E}}_{\mathrm{RS}y0}=\dfrac{1}{N}\displaystyle\sum_{k=1}^{N}y^{(k)}\\\hat{\mathrm{E}}_{\mathrm{RS}yi}\left(\theta_i\right)=\dfrac{1}{N}\displaystyle\sum_{k=1}^{N}y^{(k)}r_{\mathrm{RS}i}\left(\boldsymbol{x}^{(k)}\,|\,\theta_i,\boldsymbol{\theta}^{(k)}\right)\\\hat{\mathrm{E}}_{\mathrm{RS}yij}\left(\boldsymbol{\theta}_{ij}\right)=\dfrac{1}{N}\displaystyle\sum_{k=1}^{N}y^{(k)}r_{\mathrm{RS}ij}\left(\boldsymbol{x}^{(k)}\,|\,\boldsymbol{\theta}_{ij},\boldsymbol{\theta}^{(k)}\right)\end{cases} \tag{19}$$

where

$$\begin{cases}r_{\mathrm{RS}i}\left(\boldsymbol{x}^{(k)}\,|\,\theta_i,\boldsymbol{\theta}^{(k)}\right)=\dfrac{f_{\mathrm{X}}\left(\boldsymbol{x}^{(k)}\,|\,\theta_i,\boldsymbol{\theta}_{-i}^{(k)}\right)}{f_{\mathrm{X}}\left(\boldsymbol{x}^{(k)}\,|\,\boldsymbol{\theta}^{(k)}\right)}-1\\r_{\mathrm{RS}ij}\left(\boldsymbol{x}^{(k)}\,|\,\boldsymbol{\theta}_{ij},\boldsymbol{\theta}^{(k)}\right)=\dfrac{f_{\mathrm{X}}\left(\boldsymbol{x}^{(k)}\,|\,\boldsymbol{\theta}_{ij},\boldsymbol{\theta}_{-ij}^{(k)}\right)}{f_{\mathrm{X}}\left(\boldsymbol{x}^{(k)}\,|\,\boldsymbol{\theta}^{(k)}\right)}-\dfrac{f_{\mathrm{X}}\left(\boldsymbol{x}^{(k)}\,|\,\theta_i,\boldsymbol{\theta}_{-i}^{(k)}\right)}{f_{\mathrm{X}}\left(\boldsymbol{x}^{(k)}\,|\,\boldsymbol{\theta}^{(k)}\right)}-\dfrac{f_{\mathrm{X}}\left(\boldsymbol{x}^{(k)}\,|\,\theta_j,\boldsymbol{\theta}_{-j}^{(k)}\right)}{f_{\mathrm{X}}\left(\boldsymbol{x}^{(k)}\,|\,\boldsymbol{\theta}^{(k)}\right)}+1\end{cases}. \tag{20}$$

The variance of the estimators in Eq.(19) can be computed as:

$$\begin{cases} \mathrm{var}\left(\hat{\mathrm{E}}_{\mathrm{RS}y0}\right) \doteq \dfrac{1}{N\left(N-1\right)}\displaystyle\sum_{k=1}^{N}\left[y^{(k)2} - N\hat{\mathrm{E}}_{\mathrm{RS}y0}^{2} \right] \\ \mathrm{var}\left(\hat{\mathrm{E}}_{\mathrm{RS}yi}\right) \doteq \dfrac{1}{N\left(N-1\right)}\displaystyle\sum_{k=1}^{N}\left[y^{(k)2} r_{\mathrm{RS}i}^{2}\left(\boldsymbol{x}^{(k)} \mid \theta_i, \boldsymbol{\theta}^{(k)}\right) - N\hat{\mathrm{E}}_{\mathrm{RS}yi}^{2} \right] \\ \mathrm{var}\left(\hat{\mathrm{E}}_{\mathrm{RS}yij}\right) \doteq \dfrac{1}{N\left(N-1\right)}\displaystyle\sum_{k=1}^{N}\left[y^{(k)2} r_{\mathrm{RS}ij}^{2}\left(\boldsymbol{x}^{(k)} \mid \boldsymbol{\theta}_{ij}, \boldsymbol{\theta}^{(k)}\right) - N\hat{\mathrm{E}}_{\mathrm{RS}yij}^{2} \right] \end{cases} \tag{21}$$

The derivations of Eqs. (19)-(21) can be found in Appendix C.

Eqs. (19)-(21) indicate that, by the GEMCS method, all the RS-HDMR component functions can be easily estimated with only one set of joint samples, and the total number of *g*-function calls is *N*, which is independent of the dimensions of both input variables and their uncertain distribution parameters. The variances of the estimators can also be computed by the same set of joint samples. For each joint sample, only one or two distribution parameters take different values between the numerators and denominators of the ratio functions in Eq.(11), thus, the samples of the ratio functions in the estimators of Eq.(19) show much smaller diversity than those in Eq.(3). The above method can be easily extended to any orders of origin or central moment functions, and we don't go into further. In the following context, this method is denominated as "GEMCS-RS-HDMR".

For judging whether a RS-HDMR component function is influential or not, the Sobol' sensitivity indices can be used [31]. Due to the property of mutual orthogonality, taking variance to both sides of Eq. (4) yields,

$$\mathrm{var}_{\boldsymbol{\Theta}}\left[\mathrm{E}_y\left(\boldsymbol{\theta}\right)\right] = \sum_{i=1}^{d}\mathrm{D}_{\mathrm{E}i} + \sum_{1\le i<j\le d}\mathrm{D}_{\mathrm{E}ij} + \ldots + \mathrm{D}_{\mathrm{E}12\ldots d}\left(\boldsymbol{\theta}\right) \tag{22}$$

where $\mathrm{D}_{\mathrm{E}i} = \mathrm{var}_{\Theta_i}\left\{\mathrm{Exp}_{\boldsymbol{\Theta}_{-i}}\left[\mathrm{E}_y\left(\boldsymbol{\theta}\right) \mid \theta_i\right]\right\}$ is the first-order partial variance, $\mathrm{D}_{\mathrm{E}ij} = \mathrm{var}_{\boldsymbol{\Theta}_{ij}}\left\{\mathrm{Exp}_{\boldsymbol{\Theta}_{-ij}}\left[\mathrm{E}_y\left(\boldsymbol{\theta}\right) \mid \boldsymbol{\theta}_{ij}\right]\right\} - \mathrm{D}_{\mathrm{E}i} - \mathrm{D}_{\mathrm{E}j}$ is the second-order partial variance, etc. Based on Eq.(22), the Sobol' sensitivity index for the RS-HDMR component function $\mathrm{E}_{\mathrm{RS}yi_1i_2\ldots,i_s}\left(\boldsymbol{\theta}_{i_1i_2\ldots i_s}\right)$ is defined as [33][36]:

$$S_{\mathrm{ERS}i_1i_2\ldots,i_s} = \frac{\mathrm{D}_{\mathrm{E}i_1i_2\ldots,i_s}}{\mathrm{var}_{\boldsymbol{\Theta}}\left[\mathrm{E}_y\left(\boldsymbol{\theta}\right)\right]} \tag{23}$$

The above index possesses the property of normalization, i.e., $0 \le S_{\mathrm{ERS}i_1i_2\ldots,i_s} \le 1$. The larger this sensitivity index is, the more influential $\mathrm{E}_{\mathrm{ERS}yi_1i_2\ldots,i_s}\left(\boldsymbol{\theta}_{i_1i_2\ldots i_s}\right)$ is. If this index is lower than a threshold (e.g., 0.01), then the corresponding component function can be thought to be non-influential. This sensitivity index can also be used for estimating the truncation error of the RS-HDMR decomposition. For example, if the summation of the first-order effect indices, i.e. $\sum_{i=1}^{m} S_{\mathrm{ERSR}i}$, is very close to one, then all the interaction component functions are non-influential, and the first-order component functions are accurately enough for approximating the response expectation function.

The Sobol' sensitivity indices can be easily estimated by numerical integration procedures or by sampling techniques based the same set of joint sample points for estimating the RS-HDMR component functions, and no extra g-function call is required. Take the first-order sensitivity index $S_{\mathrm{RS}i}$ as an

example, the corresponding partial variance $\mathrm{D}_{\mathrm{E}i}$ can be derived as:

$$\mathrm{D}_{\mathrm{E}i} = \mathrm{var}_{\Theta_i}\left\{\mathrm{Exp}_{\boldsymbol{\Theta}_{\sim i}}\left[\mathrm{E}_y\left(\boldsymbol{\theta}\right)|\,\theta_i\right]\right\} \triangleq \int \hat{\mathrm{E}}^2_{\mathrm{RS}yi}\left(\theta_i\right) f_{\Theta_i}\left(\theta_i\right)\mathrm{d}\theta_i \tag{24}$$

where the estimators $\hat{\mathrm{E}}_{\mathrm{RS}yi}\left(\theta_i\right)$ and $\hat{\mathrm{E}}_{\mathrm{RS}y0}$ are the same in Eq.(19). Then, the one-dimensional integral in Eq.(24) can be estimated by any numerical integration procedure. It can also be estimated by the following estimator:

$$\hat{\mathrm{D}}_{\mathrm{E}i} = \frac{1}{N}\sum_{k=1}^{N}\hat{\mathrm{E}}^2_{\mathrm{RS}yi}\left(\boldsymbol{\theta}_i^{(k)}\right) \tag{25}$$

where $\boldsymbol{\theta}_i^{(k)}$ indicates the *k*-th sample point of θ_i drawn from the joint samples. Then, the second-order partial variances can be computed by two-dimensional numerical integration with the integrand function being $\hat{\mathrm{E}}^2_{\mathrm{RS}yij}$, or by the following estimator:

$$\hat{\mathrm{D}}_{\mathrm{E}i} = \frac{1}{N}\sum_{k=1}^{N}\hat{\mathrm{E}}^2_{\mathrm{RS}yij}\left(\boldsymbol{\theta}_{ij}^{(k)}\right) \tag{26}$$

where $\boldsymbol{\theta}_{ij}^{(k)}$ indicates the *k*-th sample point of $\boldsymbol{\theta}_{ij}$ taken from the joint samples. Higher order partial variances can be similarly estimated. The total variance $\mathrm{var}_{\boldsymbol{\Theta}}\left[\mathrm{E}_y\left(\boldsymbol{\theta}\right)\right]$ in the definition of Eq.(23) can be computed by summing all the first- and second- order partial variances, if higher order effects are not influential. In fact, estimating higher order partial variances will not introduce extra g-function calls, thus one can also estimate higher order component functions to see whether they are influential.

Generally, the GEMCS-RS-HDMR procedure has better global performance than the LEMCS-cut-HDMR procedure. These two methods can also be combined. For example, we can firstly implement the GEMCS-RS-HDMR method with small number of samples, and then reduce the estimation errors by LEMCS-cut-HDMR method if necessary. In the next section, several examples are utilized to demonstrate the performance of the two proposed methods.

5. Test examples and applications

In this section, a series of numerical and engineering examples is utilized to demonstrate the feasibility of the proposed imprecise stochastic simulation methods. For each example, we firstly compute the sensitivity indices for both the first- and second- order component functions, and thus to measure their relative importance. The non-normalized sensitivity indices are firstly computed by integrating the estimates of the corresponding component functions, and then the errors are computed by integrating the SDs of the estimated component functions, both of which are normalized by the summation of the estimates of all first two order non-normalized sensitivity indices. These two groups of results are respectively termed as “normalized sensitivity indices” and “normalized errors”, and the later one can be used for indicating the estimation error of the former one. If the summation of the sensitivity indices of several most important component functions are larger than a pre-specified threshold value (e.g., 0.97), then we conclude that the rest component functions are all non-influential. One should note that the estimations of sensitivity indices do not introduce extra g-function calls.

5.1 A toy test example

Consider a two-dimensional computational model with g-function expressed as follow:

$$y = g(\boldsymbol{x}) = 1 - \frac{(x_1 - 1)^2}{a^2} - \frac{(x_2 - 1)^3}{b^2} \tag{27}$$

where a and b are two constants, specified as 3 and 4 respectively in this application; x_1 and x_2 are two random variables following normal distribution. Due to the epistemic uncertainty, the distribution parameters of both input variables are uncertain. Their means (denoted as μ_1 and μ_2) are both uniformly distributed between -0.2 and 0.2, and their SDs (denoted as σ_1 and σ_2) are both uniformly distributed between 0.8 and 1.2. Consequently, totally four distributional parameters are investigated as $\boldsymbol{\theta} = (\theta_1, \theta_2, \theta_3, \theta_4)^T = (\mu_1, \mu_2, \sigma_1, \sigma_2)^T$. The component functions as well as the corresponding sensitivity indices are also theoretically derived for comparing the performances of the proposed two methods.

The LEMCS-cut-HDMR procedure is firstly performed for the first- and second- order origin moment functions. In this implementation, the sampling distribution parameters are fixed at their mean values, i.e., $\boldsymbol{\theta}^* = (0,0,1,1)^T$, and the samples are generated by Latin-hypercube sampling technique with sample size set to be 5000. The 95.45% confidences intervals for the constant cut-HDMR components of the first- and second- order origin moment functions are computed to be [1.012, 1.0433] and [1.3029, 1.4197], respectively. The analytical results of these two constant components are derived as 1.0278 and 1.3648, respectively, which are contained in the narrow confidence intervals, indicating that both constant components are accurately estimated.

The GEMCS-RS-HDMR procedure is subsequently performed for computing the RS-HDMR component functions of $\mathrm{E}_y(\boldsymbol{\theta})$ and $\mathrm{V}_y(\boldsymbol{\theta})$ as well as their sensitivity indices. In this implementation, the sample size is still set to be 5000, and the samples are drawn by Latin-hypercube sampling. The 95.45% confidence intervals of the constant components $\mathrm{E}_{\mathrm{RS}\,y0}$ and $\mathrm{V}_{\mathrm{RS}\,y0}$ are computed to be [1.0159, 1.0496] and [1.3428, 1.4973], and the corresponding true values analytically derived are 1.0298 and 1.4061, respectively, indicating that both constant components are accurately estimated.

The sensitivity indices defined in Eqs.(13) and (23) are computed based on the estimation of each component function. The results of the normalized first- and second- order effect indices are listed in Table 1 and Table 2, respectively, together with the analytical results, where the numbers in the superscript are the normalized errors, which are used for demonstrating the robustness of the estimated sensitivity indices. It is seen that all the sensitivity indices are accurately estimated. In Table 1, for response expectation function, all the first-order cut-HDMR and RS-HDMR component functions are significantly influential, but for second-order origin function, the first-order cut-HDMR and RS-HDMR component functions of μ_2 and σ_2 are significantly important, but those of μ_1 and σ_1 are slightly important. From Table 2, among all the second-order cut-HDMR and RS-HDMR component functions, only those of (μ_2, σ_2) show slight effect, and those of the other pairs are actually non-influential.

Table 1 The first-order sensitivity indices, where the numbers in the superscript are computed with the SDs of the estimates.

Indices	Methods	μ_1	μ_2	σ_1	σ_2
$S_{\mathrm{Ecut}\,i}$	LEMCS-cut-HDMR	$.1347^{(.0006)}$	$0.3634^{(.0017)}$	$.1366^{(.0010)}$	$.3406^{(.0099)}$
	Analytical	.1293	.3712	.1293	.3682
$S_{\mathrm{Vcut}\,i}$	LEMCS-cut-HDMR	$.0285^{(.0002)}$	$0.2663^{(.0019)}$	$.0167^{(.0003)}$	$.6615^{(.0259)}$
	Analytical	.0252	.2892	.0129	.6656
$S_{\mathrm{ERS}i}$	GEMCS-RS-HDMR	$.1140^{(.0013)}$	$.3712^{(.0036)}$	$.1533^{(.0025)}$	$.3517^{(.0146)}$
	Analytical	.1283	.3732	.1283	.3654
$S_{\mathrm{VRS}\,i}$	GEMCS-RS-HDMR	$.0255^{(.0004)}$	$.2885^{(.0039)}$	$.0091^{(.0007)}$	$.6396^{(.0309)}$
	Analytical	.0247	.2966	.0127	.6492

Table 2 The second-order sensitivity indices, where the superscripts indicates the normalized errors.

Indices	Methods	(μ_1,μ_2)	(μ_1,σ_1)	(μ_1,σ_2)	(μ_2,σ_1)	(μ_2,σ_2)	(σ_2,σ_2)
$S_{\mathrm{Ecut}\,i_1 i_2}$	LEMCS-cut-HDMR	$.0000^{(.0000)}$	$.0001^{(.0000)}$	$.0009^{(.0001)}$	$.0003^{(.0000)}$	$.0232^{(.0027)}$	$.0002^{(.0001)}$
	Analytical	.0000	.0000	.0000	.0000	.0020	.0000
$S_{\mathrm{Vcut}i_1 i_2}$	LEMCS-cut-HDMR	$.0007^{(.0000)}$	$.0011^{(.0000)}$	$.0016^{(.0003)}$	$.0005^{(.0000)}$	$.0211^{(.0024)}$	$.0020^{(.0002)}$
	Analytical	.0000	.0001	.0000	.0000	.0068	.0000
$S_{\mathrm{ERS}i_1 i_2}$	GEMCS-RS-HDMR	$.0000^{(.0001)}$	$.0014^{(.0002)}$	$.0001^{(.0004)}$	$.0001^{(.0001)}$	$.0080^{(.0014)}$	$.0003^{(.0002)}$
	Analytical	.0000	.0000	.0000	.0000	.0049	.0000
$S_{\mathrm{VRS}i_1 i_2}$	GEMCS-RS-HDMR	$.0003^{(.0001)}$	$.0015^{(.0000)}$	$.0005^{(.0007)}$	$.0002^{(.0001)}$	$.0399^{(.0035)}$	$.0010^{(.0002)}$
	Analytical	.0001	.0002	.0001	.0001	.0163	.0001

The results of first-order component functions for the first- and second- order response origin moment functions computed by the LEMCS-cut-HDMR are shown in Fig. 1 and Fig. 2 respectively, together with the analytical results. As it is shown in the figure, all the eight first-order cut-HDMR component functions are accurately estimated since the confidence intervals are narrow and contain the corresponding analytical results. For $\mathrm{E}_{\mathrm{cut}\,y4}(\sigma_4)$ and $\mathrm{V}_{\mathrm{cut}\,y4}(\sigma_4)$, the confidence intervals are wider than those of the other six component functions at the points far from $\boldsymbol{\theta}^*$, this is due to the high nonlinearity of the *g*-function w.r.t. x_2. If thinner confidence intervals need to be generated, e.g., around the point $\boldsymbol{\theta}' = (0.1, 0.1, 1.1, 1.1)$, then one can add more samples by sampling $\boldsymbol{x}$ at this fixing point.

The results of the slightly influential second-order cut-HDMR component functions of $\mathrm{E}_y(\boldsymbol{\theta})$ and $\mathrm{V}_y(\boldsymbol{\theta})$ are illustrated in Fig. 3. As can be seen, both second-order component functions are accurately estimated with very narrow confidence intervals. It is shown that the ranges of the second-order component functions are all much smaller when compared with those of the influential first-order component functions, and this has also been proved quantitatively by the sensitivity indices.

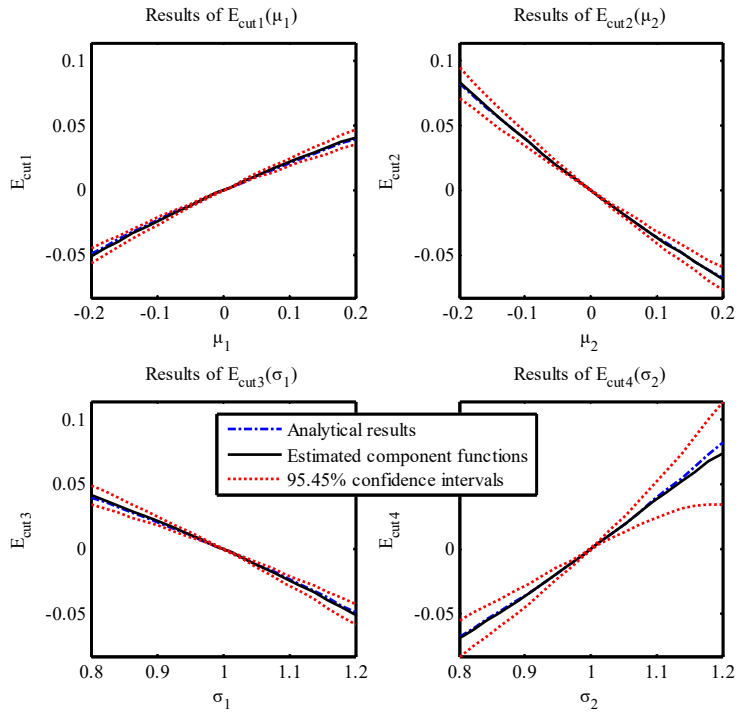

Fig. 1 The first-order cut-HDMR component functions of the response expectation function computed by the LEMCS-cut-HDMR procedure.

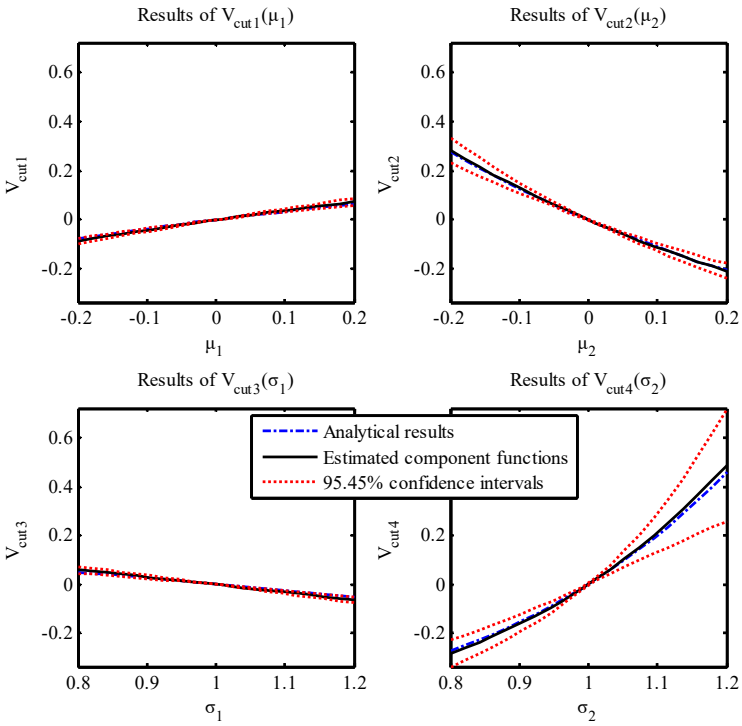

Fig. 2 The first-order component functions of the second–order origin moment functions.

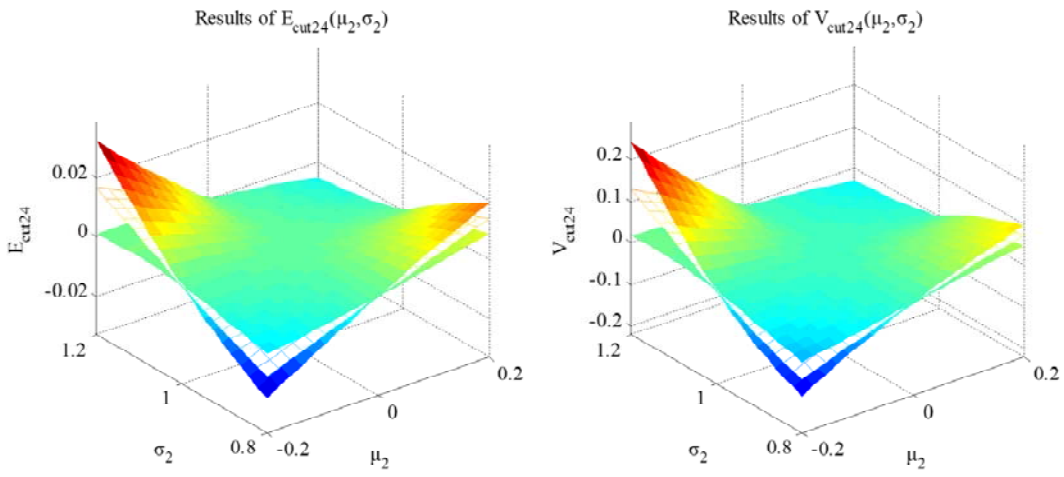

Fig. 3 The influential second-order cut-HDMR component functions of the first- and second-order response moment functions, where the in-between meshed surfaces are the estimates, the upper and lower smooth surfaces indicate the estimated 95.45% confidence intervals.

From Fig. 4-6, all the first- and second- order RS-HDMR component functions are effectively estimated with narrow confidence intervals, each of which contains the corresponding analytical result. Comparing Fig.6 with Figs.4 and 5, a qualitative conclusion is gained as all the second-order component functions are non-influential or just slightly influential. This is consistent with the conclusion drawn from the sensitivity indices in Tables 1 and 2.

From Fig. 1-3, it is observed that all the cut-HDMR component functions takes zero values at the base point or base line θ_i^*, and around these points or lines, the estimations of all the component functions are extremely accurate. Thus the LEMCS estimators have better local performance. This phenomenon is just like that of the interpolation procedure. In Fig. 4-6, the RS-HDMR component functions are not equal to zero at any points, but the estimators show good global performance. This phenomenon is similar to that of the regression technique.

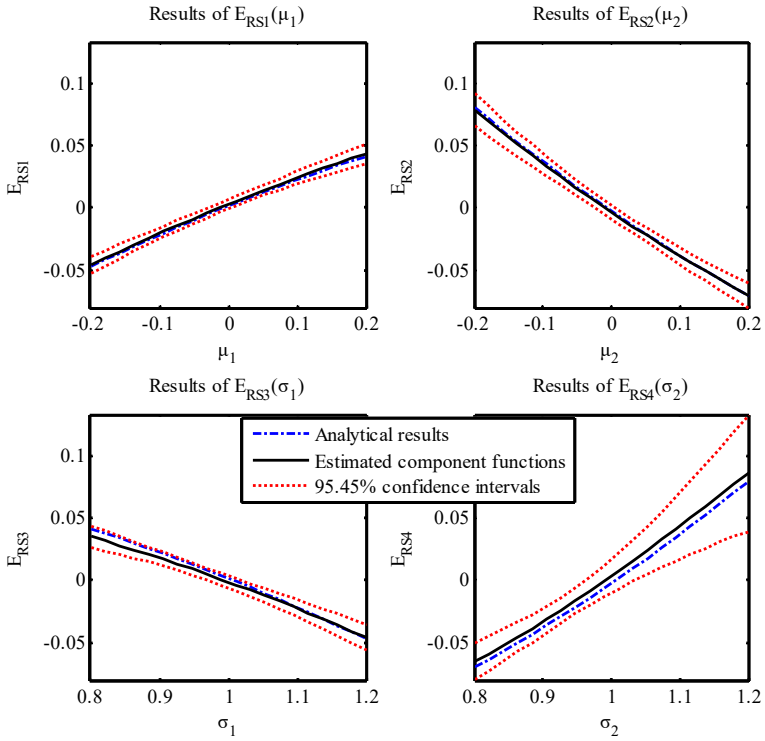

Fig. 4 The first-order RS-HDMR component functions of $\mathrm{E}_y(\boldsymbol{\theta})$ generated by the GEMCS-RS-HDMR procedure.

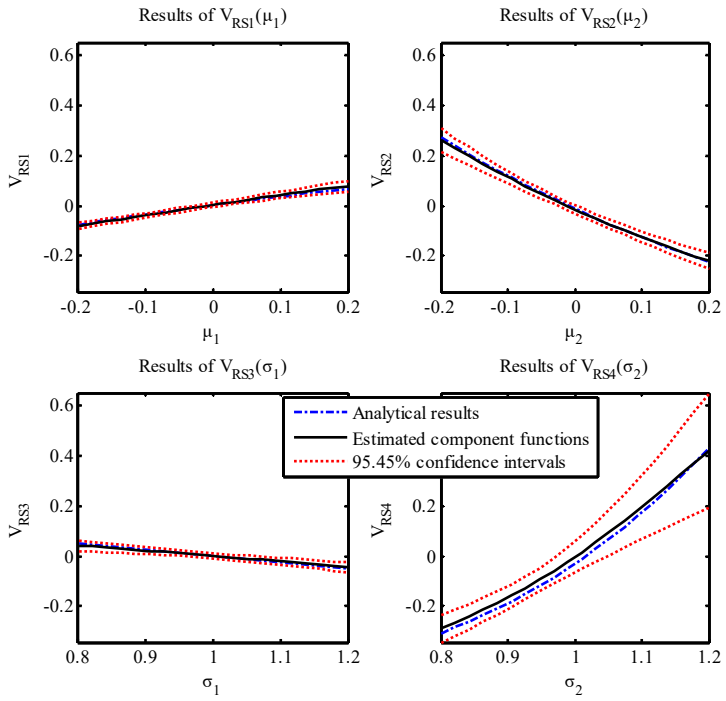

Fig. 5 The first-order RS-HDMR component functions of $\mathrm{V}_y(\boldsymbol{\theta})$.

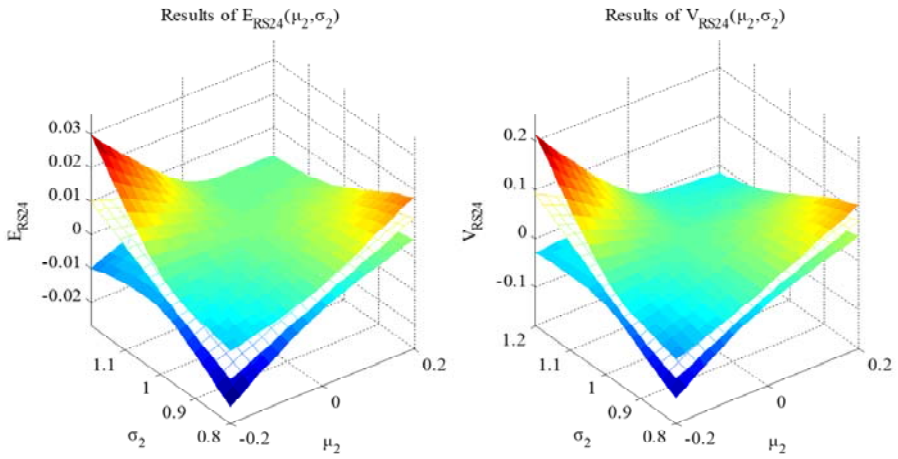

Fig. 6 The influential second-order RS-HDMR component functions of $\mathrm{E}_y(\boldsymbol{\theta})$ and $\mathrm{V}_y(\boldsymbol{\theta})$, where the in-between meshed surfaces indicate the estimates, the lower and upper surfaces refer to the 95.45% confidence intervals.

Based on the above analysis, the response expectation function $\mathrm{E}_y(\boldsymbol{\theta})$ can be approximated by the first-order cut-HDMR decomposition or the first-order RS-HDMR decomposition, i.e.,

$$\hat{\mathrm{E}}_y(\boldsymbol{\theta}) = \hat{\mathrm{E}}_{\mathrm{cut}\,y0} + \sum_{i=1}^{4} \hat{\mathrm{E}}_{\mathrm{cut}\,yi}(\theta_i) = \hat{\mathrm{E}}_{\mathrm{RS}\,y0} + \sum_{i=1}^{4} \hat{\mathrm{E}}_{\mathrm{RS}\,yi}(\theta_i).$$

The second-order origin moment function can be approximated by the first-order cut-HDMR decomposition or RS-HDMR decomposition including only the component functions of μ_2 and σ_2, i.e.,

$$\hat{\mathrm{V}}_y(\boldsymbol{\theta}) = \hat{\mathrm{V}}_{\mathrm{cut}\,y0} + \hat{\mathrm{V}}_{\mathrm{cut}\,y2}(\mu_2) + \hat{\mathrm{V}}_{\mathrm{cut}\,y4}(\sigma_2) = \hat{\mathrm{V}}_{\mathrm{RS}\,y0} + \hat{\mathrm{V}}_{\mathrm{RS}\,y2}(\mu_2) + \hat{\mathrm{V}}_{\mathrm{RS}\,y4}(\sigma_2).$$

The truncation errors must be small. The above analysis indicates that both the first- and second- order response moment functions are approximately additive w.r.t. $\boldsymbol{\theta}$. The response moment functions can also be estimated with the average estimators of LEMCS-cut-HDMR and GEMCS-RS-HDMR procedures, and this implementation makes a good balance between local and global performances.

5.2 A planar ten-bar structure

A planar ten-bar structure is shown in Fig. 7. The section area of these ten bars are all 0.001 m^2, and the length of all the vertical and horizontal bars is denoted as 'q'. The Young's module of all bars is denoted as 'E', and the three point loads, denoted as P_1, P_2 and P_3, are shown in Fig.7. The five inputs variables, i.e., q, E, P_1, P_2 and P_3, are all assumed to be normally distributed with mean values 1 m, 100GPa, 80kN, 10kN and 10kN, respectively. Due to the available information for these five parameters, the true value of their coefficients of variation (COVs) ρ_i cannot be precisely computed, and they are all bounds between 0.04 and 0.05. The model output is the vertical displacement Δ at point 3, and it is assumed that the structure fails when Δ exceeds 0.0035 m. For this test example, the mean value of Δ nearly does not change w.r.t. the COVs of each input variables in their support bounds, thus we estimate the second-order origin moment function of the limit state function and the failure probability function

w.r.t. the COVs of each input. The g-function can be generated analytically (see Ref. [27]), or simulated by FE model. Here, a FE model established in Ansys is used.

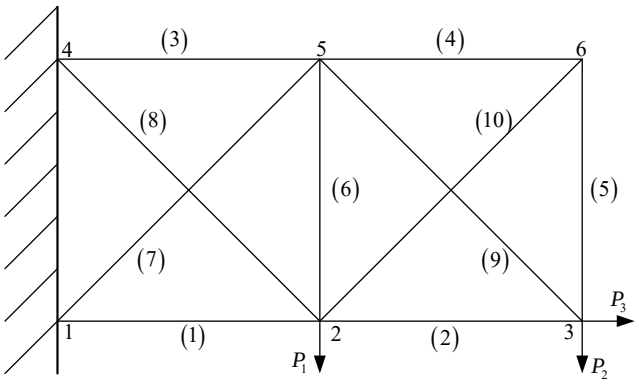

Fig. 7 A planar ten-bar structure.

The sensitivity indices of the cut-HDMR and RS-HDMR component functions for the second-order moment function and the failure probability function are evaluated with 1e4 sample points, and the results are shown in Tables 3 and 4 respectively, where the superscripts indicate the results computed with the SDs of the estimates of the corresponding component functions. As it is shown in the tables, the variation of each estimated sensitivity index is small, implying that the sensitivity indices are accurately estimated. From the sensitivity indices it can be concluded that all the second-order cut-HDMR and RS-HDMR component functions are non-influential, and among the five first-order component functions, only those of q, E and P_1 are influential. Compared with P_1, the component functions of P_2 and P_3 are not influential because their realizations are much small than that of P_1. Thus, whether the second-order moment function or the failure probability function are considered, only the constant components and three first-order component functions need to be estimated.

With the same sets of samples, the constant HDMR components are computed, and the results are reported in the last row of Table 3, where the superscripts indicate the SDs of the estimates. As can be seen, they are all accurately computed. The influential HDMR component functions are then computed, and the results are illustrated in Figs.8 and 9. As their estimators are unbiased and the SDs are small, the results are accurate and robust.

Table 3 The first-order sensitivity indices of the ten-bar structure, where the superscripts indicate the corresponding normalized errors.

Methods	LEMCS-cut-HDMR		GEMCS-RS-HDMR	
Indices	$S_{\mathrm{V}\mathrm{cut}\,i}$	$S_{\mathrm{P}_f\mathrm{cut}\,i}$	$S_{\mathrm{VRS}i}$	$S_{\mathrm{P}_f\mathrm{RS}i}$
q	$.4426^{(.0143)}$	$.3113^{(.0031)}$	$.4575^{(.0199)}$	$.2492^{(.0071)}$
E	$.3448^{(.0101)}$	$.5144^{(.0043)}$	$.2711^{(.0180)}$	$.6222^{(.0080)}$
P_1	$.1967^{(.0095)}$	$.1725^{(.0026)}$	$.2548^{(.0329)}$	$.1170^{(.0073)}$
P_2	$.0016^{(.0062)}$	$.0014^{(.0012)}$	$.0025^{(.0110)}$	$.0052^{(.0021)}$
P_3	$.0136^{(.0053)}$	$.0003^{(.0012)}$	$.0104^{(.0100)}$	$.0045^{(.0023)}$
Constant components	$1.972\text{e-}7^{(2.384\text{e-}9)}$	$.0412^{(.0021)}$	$1.917\text{e-}7^{(1.917\text{e-}9)}$	$.0433^{(.0020)}$

Table 4 The second-order sensitivity indices of the ten-bar structure, where the results in the superscripts are computed with the SDs of the estimators of the corresponding component functions.

Methods	LEMCS-cut-HDMR		GEMCS-RS-HDMR	
Indices	$S_{\mathrm{V}\mathrm{cut}ij}$	$S_{\mathrm{P}_f\mathrm{cut}ij}$	$S_{\mathrm{VRS}ij}$	$S_{\mathrm{P}_f\mathrm{RS}ij}$
(q,E)	$.0000^{(.0002)}$	$.0000^{(.0000)}$	$.0003^{(.0004)}$	$.0001^{(.0001)}$
(q,P_1)	$.0000^{(.0002)}$	$.0001^{(.0001)}$	$.0010^{(.0009)}$	$.0004^{(.0002)}$
(q,P_2)	$.0000^{(.0002)}$	$.0000^{(.0000)}$	$.0001^{(.0002)}$	$.0001^{(.0001)}$
(q,P_3)	$.0001^{(.0001)}$	$.0000^{(.0001)}$	$.0005^{(.0003)}$	$.0000^{(.0001)}$
(E,P_1)	$.0002^{(.0001)}$	$.0000^{(.0000)}$	$.0004^{(.0007)}$	$.0004^{(.0001)}$
(E,P_2)	$.0003^{(.0001)}$	$.0000^{(.0000)}$	$.0002^{(.0005)}$	$.0001^{(.0001)}$
(E,P_3)	$.0000^{(.0001)}$	$.0000^{(.0000)}$	$.0005^{(.0004)}$	$.0001^{(.0002)}$
(P_1,P_2)	$.0000^{(.0001)}$	$.0000^{(.0000)}$	$.0003^{(.0004)}$	$.0001^{(.0001)}$
(P_1,P_3)	$.0000^{(.0001)}$	$.0000^{(.0000)}$	$.0002^{(.0006)}$	$.0001^{(.0001)}$
(P_2,P_3)	$.0001^{(.0000)}$	$.0000^{(.0000)}$	$.0001^{(.0002)}$	$.0002^{(.0000)}$

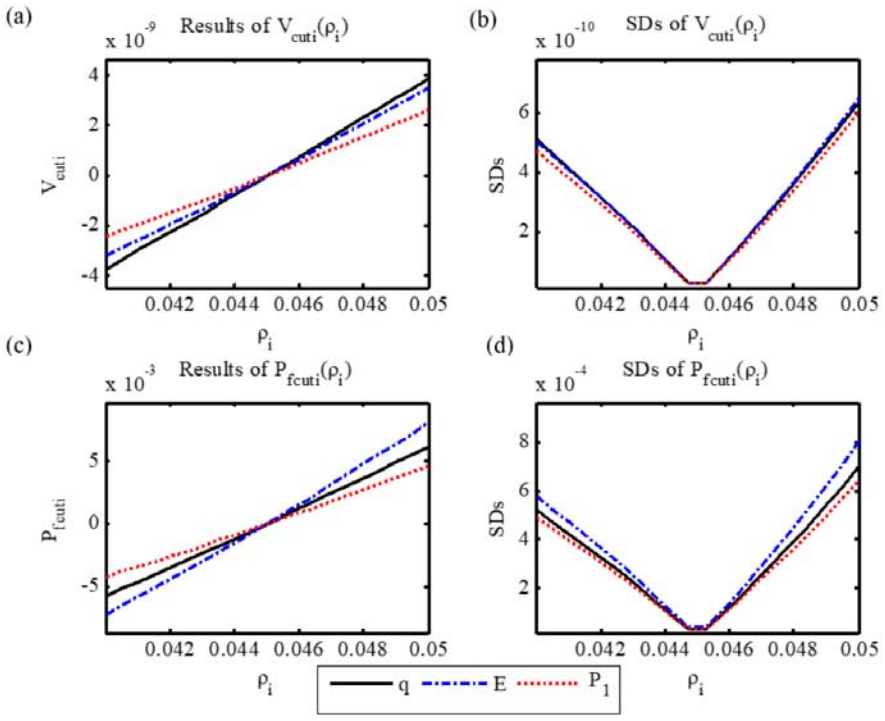

Fig. 8 The influential cut-HDMR component functions of the ten-bar structure.

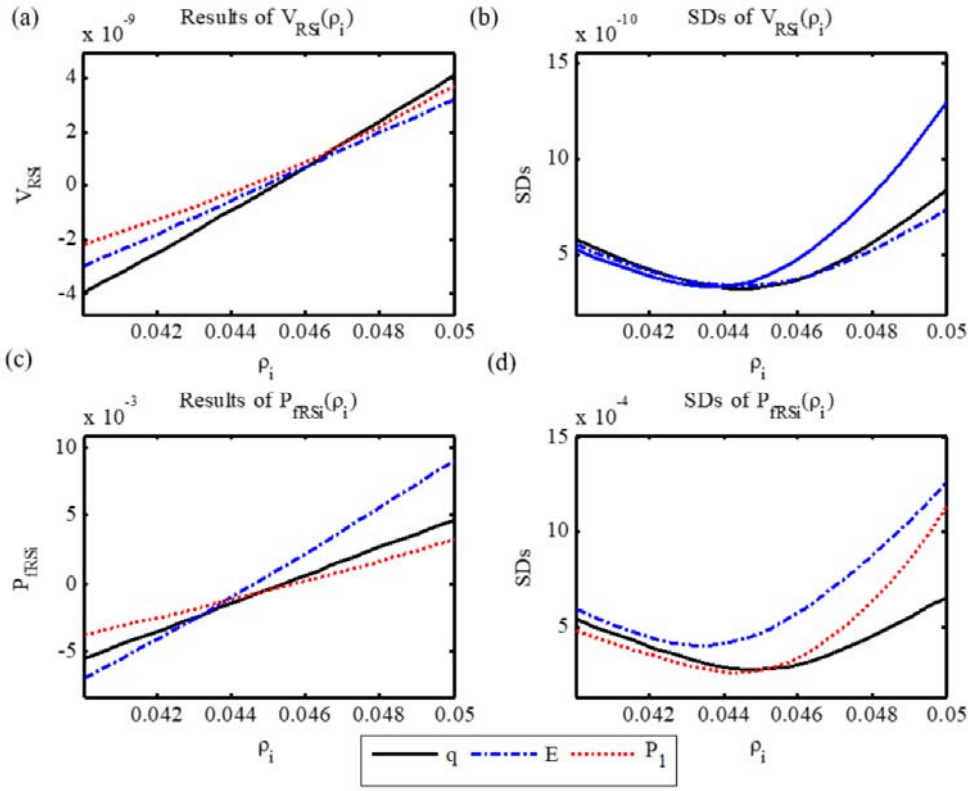

Fig. 9 The influential RS-HDMR component functions of the ten-bar structure

5.3 A simplified wing-box model

A simplified wing-box structure used on aircraft is proposed in this example as shown in Fig.10, and a FE model of this structure is developed for the following calculation [27]. The wing structure consists of 16 plates and 28 bars. The 28 bars are divided into three groups based on their direction, and the lengths of the bars in *X*, *Y* and Z directions are denoted as L_X, L_Y and L_Z respectively. The section areas of all bars are assumed to be the same and are denoted as *A*. The thicknesses of all plates are also assumed to be the same, and are denoted as *TH*. The elastic modulus of all components are denoted as *E*, and the Poisson's ratio of all components are assumed to be 0.3. The distributed load is simplified to six point loads, and are scaled by the parameter *P*, as shown in Fig.10. All the seven input variables are assumed to be normal random variables with distribution parameters as detailed in Table 5. The relative vertical displacement Δ_{16} at the 16th points is assumed to be the model output, and the limit state function is defined by $g = 0.003\text{m} - \Delta_{16}$. One should note that, for each input simulation sample, the relative displacement Δ_{16} is measured as the distance between the positions of node 16 after and before performing the loads, instead of the position of node 16. The aim of this example is to estimate the second-order origin moment function and the failure probability function.

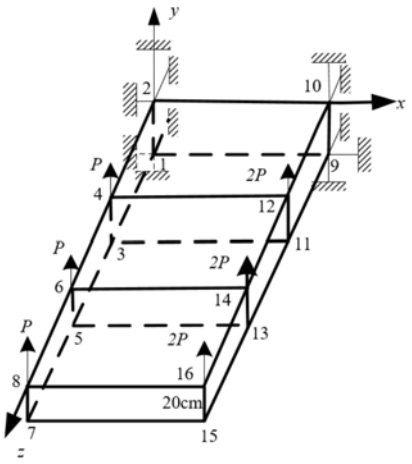

Fig. 10 A simplified wing-box model

Table 5 Distribution parameters of the input variables of the wing-box model

Variables	A	L_X	L_Y	L_Z	E	P	TH
means	1e-3 m^2	0.6 m	0.2 m	0.4 m	7.1×10^{10} Pa	1500 N	0.003 m
COVs	[0.08, 0.12]						

The calculation time of each FE model running is about 12 seconds, and totally 3000 FE samples are executed for each method implement. The first-order sensitivity indices for both cut-HDMR and RS-HDMR component functions are detailed in Table 6, and since all the second-order sensitivity indices are very small, we don't display the results. The influential first-order component functions can be easily identified by these sensitivity indices, and the results of those influential ones are plotted in Fig. 11 and Fig. 12. It is shown that, all the influential component functions are accurately estimated around the nominal values of the COVs (i.e., 0.1), while around the end points, the SDs of the estimates are relatively large.

Table 6 Results of the sensitivity indices for the wing-box model, where the superscripts are computed based on the SDs of the HDMR component functions.

Methods	LEMCS-cut-HDMR		GEMCS-RS-HDMR	
Indices	$S_{\mathrm{V}\mathrm{cut}i}$	$S_{\mathrm{P}_f\mathrm{cut}i}$	$S_{\mathrm{VRS}i}$	$S_{\mathrm{P}_f\mathrm{RS}i}$
A	$.0001^{(.0132)}$	$.0016^{(.0024)}$	$.0297^{(.0340)}$	$.0074^{(.0109)}$
L_X	$.0003^{(.0117)}$	$.0001^{(.0031)}$	$.0074^{(.0230)}$	$.0056^{(.0065)}$
L_Y	$.4230^{(.0332)}$	$.4179^{(.0120)}$	$.4080^{(.0425)}$	$.3767^{(.0152)}$
L_Z	$.4845^{(.0523)}$	$.5585^{(.0147)}$	$.4530^{(.0445)}$	$.4863^{(.0174)}$
E	$.0574^{(.0255)}$	$.0076^{(.0045)}$	$.0245^{(.0393)}$	$.0560^{(.0164)}$
P	$.0015^{(.0141)}$	$.0009^{(.0030)}$	$.0133^{(.0276)}$	$.0340^{(.0163)}$
TH	$.0100^{(.0150)}$	$.0088^{(.0047)}$	$.0013^{(.0232)}$	$.0023^{(.0063)}$
Constant components	$3.970\text{e-}6^{(6.005\text{e-}8)}$	$6.667\text{e-}2^{(4.555\text{e-}3)}$	$4.015\text{e-}6^{(7.330\text{e-}8)}$	$7.100\text{e-}2^{(4.689\text{e-}3)}$

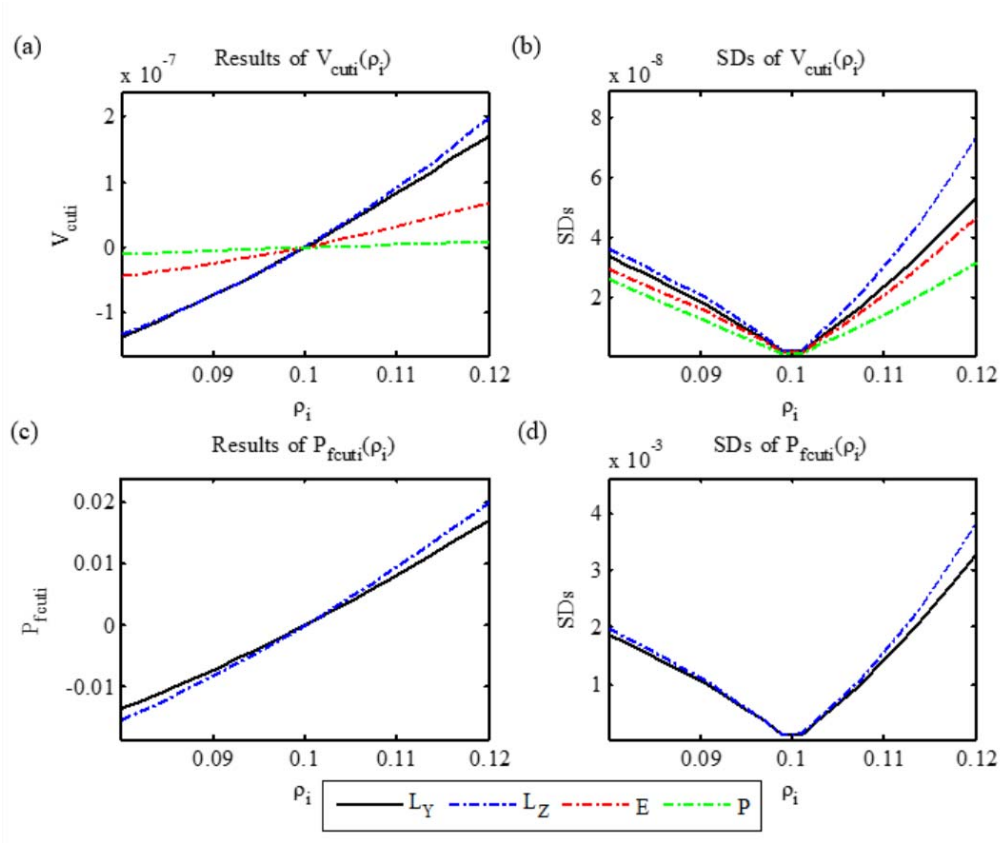

Fig. 11 Results of the first-order cut-HDMR component functions of the wing-box model.

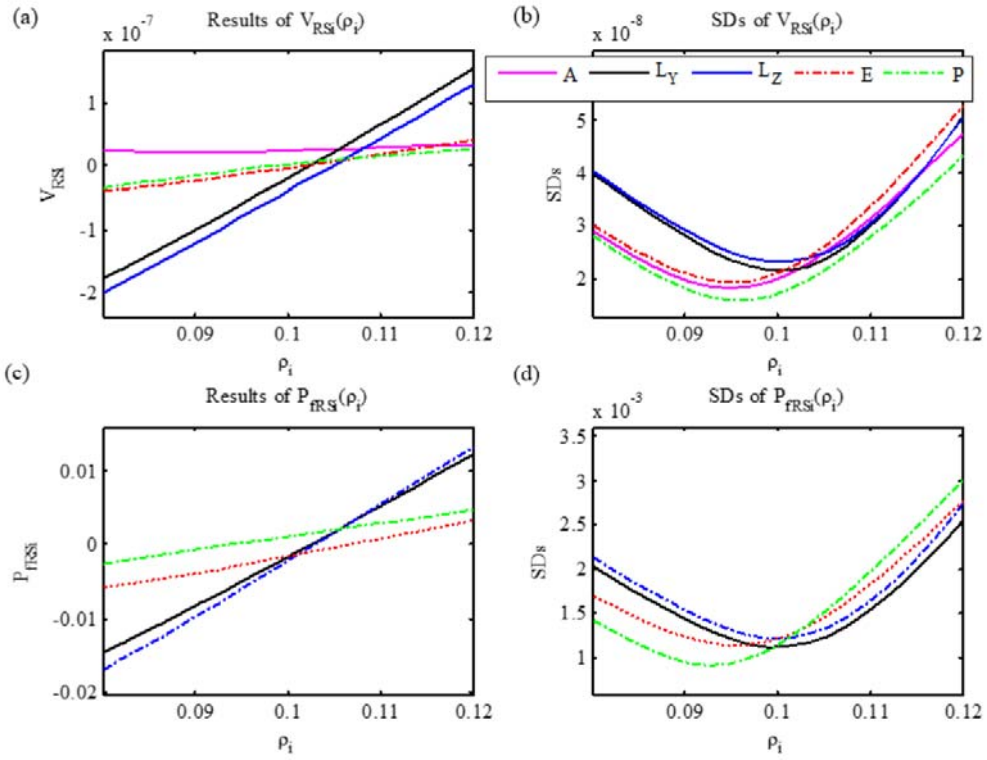

Fig. 12 Results of the RS-HDMR component functions of the wing-box model.

6. Discussions and conclusions

This set of companion papers presents a new general framework, called *non-intrusive imprecise stochastic simulation*, for uncertainty propagation of the parameterized imprecise probability models through computational models, and specifically, in this paper, the performance estimation is concerned. Due to the poor performance of the classical LEMCS procedure in high dimension, the HDMR decomposition method is proposed for improving the performance. The GEMCS method is firstly developed for improving the global performance of EMCS method, where a pre-assigned sampling point $\boldsymbol{\theta}^*$ is no longer required. Then, due to the local property of both LEMCS and cut-HDMR procedures, they are combined to form a new method termed as LEMCS-cut-HDMR with the purpose to sufficiently improve the accuracy in high dimension. What's more, due to the global property of both GEMCS and RS-HDMR procedures, they are combined to form a new procedure called GEMCS-RS-HDMR. In both methods, the confidence intervals are derived for all component functions, and sensitivity indices are introduced for analyzing the truncation errors as well as the influential component functions.

The performance of the proposed framework has been verified by several numerical and engineering examples. It is shown that the LEMCS-cut-HDMR method has feasible local performance, while the GEMCS-RS-HDMR method has better global performance, and these two methods can also be combined such that a balance between the global and local performances can be achieved.

Compared with the traditional methods for uncertainty propagation of imprecise probability models (e.g., those reported in Refs. [11] and [15]), the developed imprecise stochastic simulation framework successfully avoids performing optimization on the g-function, which is commonly quite computationally expensive and difficult to obtain a global convergence especially when the g-function is non-convex. The second advantage of the developed framework is that all the involved methods are non-intrusive, thus can be applied to any black-box model. The third advantage is that, all the precise stochastic simulation procedures (such as importance sampling [22], line sampling [23] and subset simulation [24]) can be injected into the framework. There are two main disadvantages. Firstly, compared with the used precise stochastic simulation procedure, the imprecise stochastic simulation estimators commonly have larger variances especially when the support of $\boldsymbol{\theta}$ is large, but this may be relieved by variate control techniques, which will be specifically treated in further development. Secondly, the current version of the developed framework is not applicable for non-parameterized imprecise probability models such as free p-box model, but this extension will be conducted in future work.

As imprecise probability models have been regarded as the competitive models for handling aleatory and epistemic uncertainties separately when the available information is incomplete and/or imprecise, the proposed framework provides a solid footstone for further theory study in, e.g., reliability analysis [错误!未找到引用源。], sensitivity analysis [28], Bayesian model updating [38], etc., in mixed uncertainties environment.

The proposed framework can also be used for estimating failure probability function w.r.t. the input distribution parameters, however, as it will be shown in the companion paper, this framework is only applicable when the failure probability is large. For rare failure events frequently encountered in real engineering applications, this framework cannot be directly used. The companion paper concentrates on this specific problem.

Appendix A: Proof of the GEMCS estimators

Let $\boldsymbol{\theta}'$ indicate a random replication of $\boldsymbol{\theta}$, then the response expectation function $\mathrm{E}_y(\boldsymbol{\theta})$ can be derived as:

$$\begin{aligned}\mathrm{E}_y(\boldsymbol{\theta}) &= \int g(\boldsymbol{x}) f_{\mathrm{X}}(\boldsymbol{x}\mid\boldsymbol{\theta})\mathrm{d}\boldsymbol{x} = \int g(\boldsymbol{x}) f_{\mathrm{X}}(\boldsymbol{x}\mid\boldsymbol{\theta})\, f_{\Theta}(\boldsymbol{\theta}')\mathrm{d}\boldsymbol{x}\mathrm{d}\boldsymbol{\theta}' \\ &= \int g(\boldsymbol{x})\frac{f_{\mathrm{X}}(\boldsymbol{x}\mid\boldsymbol{\theta})}{f_{\mathrm{X}}(\boldsymbol{x}\mid\boldsymbol{\theta}')} f_{\Theta}(\boldsymbol{\theta}')\, f_{\mathrm{X}}(\boldsymbol{x}\mid\boldsymbol{\theta}')\mathrm{d}\boldsymbol{x}\mathrm{d}\boldsymbol{\theta}' \\ &= \int g(\boldsymbol{x})\frac{f_{\mathrm{X}}(\boldsymbol{x}\mid\boldsymbol{\theta})}{f_{\mathrm{X}}(\boldsymbol{x}\mid\boldsymbol{\theta}')} f_{\mathrm{X},\Theta}(\boldsymbol{x},\boldsymbol{\theta}')\mathrm{d}\boldsymbol{x}\mathrm{d}\boldsymbol{\theta}'\end{aligned} \tag{A1}$$

Then given a set of joint samples $\left(\boldsymbol{x}^{(k)},\boldsymbol{\theta}^{(k)}\right)$ $(k=1,2,\ldots,N)$ following joint PDF $f_{\mathrm{X},\Theta}(\boldsymbol{x},\boldsymbol{\theta}')$, an unbiased estimator of $\mathrm{E}_y(\boldsymbol{\theta})$ can be derived as:

$$\mathrm{E}_y(\boldsymbol{\theta}) = \frac{1}{N}\sum_{k=1}^{N} g(\boldsymbol{x})\frac{f_{\mathrm{X}}(\boldsymbol{x}^{(k)}\mid\boldsymbol{\theta})}{f_{\mathrm{X}}(\boldsymbol{x}^{(k)}\mid\boldsymbol{\theta}^{(k)})} \tag{A2}$$

The GEMCS estimators for $\mathrm{V}_y(\boldsymbol{\theta})$ and $\mathrm{P}_f(\boldsymbol{\theta})$ can be similarly derived.

Appendix B: Derivations for LEMCS-cut-HDMR procedure

The constant cut-HDMR component $\mathrm{E}_{\mathrm{cut}y0}$ in Eq.(5) can be derived as:

$$\mathrm{E}_{\mathrm{cut}\,y0} = \int g(\boldsymbol{x}) f_{\mathrm{X}}(\boldsymbol{x}\mid\boldsymbol{\theta}^*)\mathrm{d}\boldsymbol{x} = \mathrm{Exp}_{\boldsymbol{\theta}^*}\left[g(\boldsymbol{x})\right]. \tag{A3}$$

Similarly, the first- and second order component functions in Eqs. (6) and (7) can be formulated as:

$$\mathrm{E}_{\mathrm{cut}\,yi}\left(\theta_i,\boldsymbol{\theta}^*_{-i}\right) = \int g(\boldsymbol{x})\left[\frac{f_{\mathrm{X}}(\boldsymbol{x}\mid\theta_i,\boldsymbol{\theta}^*_{-i})}{f_{\mathrm{X}}(\boldsymbol{x}\mid\boldsymbol{\theta}^*)}-1\right] f_{\mathrm{X}}(\boldsymbol{x}\mid\boldsymbol{\theta}^*)\mathrm{d}\boldsymbol{x} - \mathrm{E}_{y0} = \mathrm{Exp}_{\boldsymbol{\theta}^*}\left[g(\boldsymbol{x}) r_{\mathrm{cut}\,i}(\boldsymbol{x}\mid\theta_i,\boldsymbol{\theta}^*)\right] \tag{A4}$$

and

$$\begin{aligned}\mathrm{E}_{\mathrm{cut}\,yij}\left(\boldsymbol{\theta}_{ij}\right) &= \int g(\boldsymbol{x})\left[\frac{f_X(\boldsymbol{x}\mid\theta_{ij},\boldsymbol{\theta}^*_{-ij})}{f_X(\boldsymbol{x}\mid\boldsymbol{\theta}^*)} - \frac{f_X(\boldsymbol{x}\mid\theta_i,\boldsymbol{\theta}^*_{-i})}{f_X(\boldsymbol{x}\mid\boldsymbol{\theta}^*)} - \frac{f_X(\boldsymbol{x}\mid\theta_j,\boldsymbol{\theta}^*_{-j})}{f_X(\boldsymbol{x}\mid\boldsymbol{\theta}^*)} - 1\right] f_X(\boldsymbol{x}\mid\boldsymbol{\theta}^*)\mathrm{d}\boldsymbol{x} \\ &= \mathrm{Exp}_{\boldsymbol{\theta}^*}\left[g(\boldsymbol{x}) r_{\mathrm{cut}\,ij}(\boldsymbol{x}\mid\theta_{ij},\boldsymbol{\theta}^*)\right].\end{aligned} \tag{A5}$$

Then, based on one set of samples $\boldsymbol{x}^{(k)}$ $(k=1,2,\ldots,N)$ generated from $f_X(\boldsymbol{x}\mid\boldsymbol{\theta}^*)$ as well as the corresponding values $y^{(k)} = g\left(\boldsymbol{x}^{(k)}\right)$ of model response, the three component functions can be estimated by:

$$\begin{cases}\hat{\mathrm{E}}_{\mathrm{cut}\,y0}\left(\boldsymbol{\theta}^*\right) = \dfrac{1}{N}\displaystyle\sum_{k=1}^{N} y^{(k)} \\ \hat{\mathrm{E}}_{\mathrm{cut}\,yi}\left(\theta_i,\boldsymbol{\theta}^*_{-i}\right) = \dfrac{1}{N}\displaystyle\sum_{k=1}^{N} y^{(k)} r_{\mathrm{cut}\,i}\left(\boldsymbol{x}^{(k)}\mid\theta_i,\boldsymbol{\theta}^*\right) \\ \hat{\mathrm{E}}_{\mathrm{cut}\,yij}\left(\boldsymbol{\theta}_{ij},\boldsymbol{\theta}^*_{-ij}\right) = \dfrac{1}{N}\displaystyle\sum_{k=1}^{N} y^{(k)} r_{\mathrm{cut}\,ij}\left(\boldsymbol{x}^{(k)}\mid\boldsymbol{\theta}_{ij},\boldsymbol{\theta}^*\right)\end{cases}. \tag{A6}$$

It is easy to prove that the three estimators in Eq.(A6) are all unbiased. The variance of the estimator $\hat{\mathrm{E}}_{\mathrm{cut}\,y0}$ can be derived as:

$$\mathrm{var}\left(\hat{\mathrm{E}}_{\mathrm{cut}\,y0}\right)=\frac{1}{N^2}\sum_{j=1}^{N}\mathrm{var}\left[y^{(k)}\right]=\frac{1}{N}\mathrm{var}\left[y^{(k)}\right]\hat{=}\frac{1}{N\left(N-1\right)}\sum_{k=1}^{N}\left[y^{(k)2}-N\hat{\mathrm{E}}_{\mathrm{cut}\,y0}^{2}\right] \tag{A7}$$

And similarly, the variances of the estimators $\hat{\mathrm{E}}_{\mathrm{cut}\,yi}$ and $\hat{\mathrm{E}}_{\mathrm{cut}\,yij}$ can be derived as:

$$\begin{cases}\mathrm{var}\left(\hat{\mathrm{E}}_{\mathrm{cut}\,yi}\right)\hat{=}\dfrac{1}{N\left(N-1\right)}\left\{\sum_{k=1}^{N}y^{(k)2}r_{\mathrm{cut}\,i}^{2}\left(\boldsymbol{x}^{(k)}\mid\theta_i,\boldsymbol{\theta}^{*}\right)-N\hat{\mathrm{E}}_{\mathrm{cut}\,yi}^{2}\right\}\\ \mathrm{var}\left(\hat{\mathrm{E}}_{\mathrm{cut}\,yij}\right)\hat{=}\dfrac{1}{N\left(N-1\right)}\left\{\sum_{k=1}^{N}y^{(k)2}r_{\mathrm{cut}\,ij}^{2}\left(\boldsymbol{x}^{(k)}\mid\boldsymbol{\theta}_{ij},\boldsymbol{\theta}^{*}\right)-N\hat{\mathrm{E}}_{\mathrm{cut}\,yij}^{2}\right\}\end{cases} \tag{A8}$$

By replacing $y^{(k)}$ in Eqs. (A6)-(A8) with $y^{(k)2}$, we can easily obtain the estimators for the cut-HDMR component functions of the second-order response origin moment functions as well as their variances. Higher order component functions can also be derived in the same way.

■

Appendix C: Derivatives for GEMCS-RS-HDMR procedure

Let $\left(\boldsymbol{x}^{(k)},\boldsymbol{\theta}^{(k)}\right)$ ($k=1,2,\ldots,N$) denote the joint sample generated from $f_{\boldsymbol{X},\boldsymbol{\Theta}}\left(\boldsymbol{x},\boldsymbol{\theta}\right)$, and $y^{(k)}=g\left(\boldsymbol{x}^{(k)}\right)$ indicates the corresponding values of model response. Then, when $\boldsymbol{\theta}$ is fixed at $\boldsymbol{\theta}^{(k)}$, similar to the derivation of Eq.(A6), $y^{(k)}$, $y^{(k)}r_{\mathrm{RS}i}\left(\boldsymbol{x}^{(k)}\mid\theta_i,\boldsymbol{\theta}^{(k)}\right)$ and $y^{(k)}r_{\mathrm{RS}ij}\left(\boldsymbol{x}^{(k)}\mid\boldsymbol{\theta}_{ij},\boldsymbol{\theta}^{(k)}\right)$ are respectively the unbiased estimator of $\mathrm{E}_{\mathrm{RS}\,y0}\left(\boldsymbol{\theta}^{(k)}\right)$, $\mathrm{E}_{\mathrm{RS}\,yi}\left(\theta_i,\boldsymbol{\theta}_i^{(k)}\right)$ and $\mathrm{E}_{\mathrm{RS}\,yij}\left(\boldsymbol{\theta}_{ij},\boldsymbol{\theta}_{ij}^{(k)}\right)$. Thus, the unbiased estimators for the RS-HDMR component functions in Eqs.(14)-(16) can be derived as the average values of these three estimators across all samples of $\boldsymbol{\theta}$, i.e., :

$$\begin{cases}\hat{\mathrm{E}}_{\mathrm{RS}0}=\dfrac{1}{N}\sum_{k=1}^{N}y^{(k)}\\ \hat{\mathrm{E}}_{\mathrm{RS}i}\left(\theta_i\right)=\dfrac{1}{N}\sum_{k=1}^{N}y^{(k)}r_{\mathrm{RS}i}\left(\boldsymbol{x}^{(k)}\mid\theta_i,\boldsymbol{\theta}^{(k)}\right)\\ \hat{\mathrm{E}}_{\mathrm{RS}ij}\left(\boldsymbol{\theta}_{ij}\right)=\dfrac{1}{N}\sum_{k=1}^{N}y^{(k)}r_{\mathrm{RS}ij}\left(\boldsymbol{x}^{(k)}\mid\boldsymbol{\theta}_{ij},\boldsymbol{\theta}^{(k)}\right)\end{cases}. \tag{A9}$$

As $y^{(k)}$ ($k=1,2,\ldots,N$) are independent identically distributed, the variance of the estimators $\hat{\mathrm{E}}_{\mathrm{RS}0}$ is derived as follows:

$$\mathrm{var}\left(\hat{\mathrm{E}}_{\mathrm{RS}\,0}\right)=\frac{1}{N}\mathrm{var}\left[y^{(k)}\right]\hat{=}\frac{1}{N\left(N-1\right)}\sum_{k=1}^{N}\left[y^{(k)2}-N\hat{\mathrm{E}}_{\mathrm{RS}\,0}\right] \tag{A10}$$

Similarly, the variances of the estimators $\hat{\mathrm{E}}_{\mathrm{RS}i}$ and $\hat{\mathrm{E}}_{\mathrm{RS}yij}$ are derived as:

$$\begin{cases}\mathrm{var}\left(\hat{\mathrm{E}}_{\mathrm{RS}\,yi}\right)\hat{=}\dfrac{1}{N\left(N-1\right)}\sum_{k=1}^{N}\left[y^{(k)2}r_{\mathrm{RS}i}^{2}\left(\boldsymbol{x}^{(k)}\mid\theta_i,\boldsymbol{\theta}^{(k)}\right)-N\hat{\mathrm{E}}_{\mathrm{RS}\,yi}\right]\\ \mathrm{var}\left(\hat{\mathrm{E}}_{\mathrm{RS}\,yij}\right)\hat{=}\dfrac{1}{N\left(N-1\right)}\sum_{k=1}^{N}\left[y^{(k)2}r_{\mathrm{RS}ij}^{2}\left(\boldsymbol{x}^{(k)}\mid\boldsymbol{\theta}_{ij},\boldsymbol{\theta}^{(k)}\right)-N\hat{\mathrm{E}}_{\mathrm{RS}\,yij}\right]\end{cases} \tag{A11}$$

The estimators of the RS-HDMR component functions of the second-order response origin moment functions as well as the variances can be similarly derived.

■

Acknowledgements

This work is supported by the Natural Science Basic Research Plan in Shaanxi Province of China (Grant No. 2017JQ1007) and Aerospace Science and Technology Foundation of China. The first author is also supported by the Top International University Visiting Program for Outstanding Young scholars of Northwestern Polytechnical University. The first and third authors are both supported by the Alexander von Humboldt Foundation of Germany. The second author is supported by the program of China Scholarships Council (CSC). Part of this work is supported by the National Natural Science Foundation of China (Grant No. U1530122). The authors are thankful for all these grants.

Reference

[1] A. Der Kiureghian, O. Ditlevsen, Aleatory or epistemic? Does it matter? Struct. Saf. 31 (2009) 105-112

[2] M. Beer, S. Ferson, V. Kreinovich, Imprecise probabilities in engineering analyses, Mech. Syst. Signal Process. 37 (2013) 4-29

[3] E. Patelli, D.A. Albarez, M. Broggi, M. De Angelis, Uncertainty management in multidisciplinary design of critical safety systems, J. Aerosp. Inf. Syst. 12 (2015) 140-169

[4] C.Jiang, R.G. Bi, G.Y. Lu, X. Han, Structural reliability analysis using non-probabilistic convex model, Comput. Method Appl. M. 254(2013) 83-98.

[5] J.C. Helton, J.D. Johnson, W.L. Oberkampf, C.J. Sallaberry, Representation of analysis results involving aleatory and epistemic uncertainty, Int. J. Gen. Syst. 39 (2010) 605-646.

[6] J.E. Oakley, A. O'Hagan, Probabilistic sensitivity analysis of complex models: a Bayesian approach, J. R. Stat. Soc. B (Statistical Methodol.) 66 (2004) 751-769

[7] K. Sentz, S. Ferson, Combination of evidence in Dempster-Shafer theory, Livermore, California: Sandia National Laboratories, 2002

[8] S. Sun, G. Fu, S. Djordjević, S.T. Khu, Separating aleatory and epistemic uncertainties: Probabilistic sewer flooding evaluation using probability box, J. Hydrol. 420 (2012) 360-372.

[9] M. Stein, M. Beer, V. Kreinovich, Bayesian approach for inconsistent information, Inform. Sciences 245(2013) 96-111

[10] S. Sankararaman, S. Mahadevan, Likelihood-based representation of epistemic uncertainty due to sparse point data and/or interval data, Reliab. Eng. Syst. Safe. 96 (2011) 814-824.

[11] D.A. Alvarez, F. Uribe, J.E. Hurtado, Estimation of the lower and upper bounds on the probability of failure using subset simulation and random set theory, Mech. Syst. Signal Process 100 (2018) 782-801

[12] A.M. Hasofer, N.C. Lind, An exact and invariant first order reliability format, J. Eng. Mech. 100 (1974) 111-121.

[13] I. Lee, Y. Noh, D. Yoo, A novel second-order reliability method (SORM) using noncentral or generalized chi-squared distribution, J. Mech. Design 134 (2012) 100912

[14] Y.G. Zhao, X.Y. Zhang, Z.H. Lu, Complete monotonic expression of the fourth-moment normal transformation for structural reliability, Comput. Struct. 196 (2018) 186-199.

[15] Z. Zhang, C. Jiang, G.G. Wang, X. Han, First and second order approximate reliability analysis methods using evidence theory, Reliab. Eng. Syst. Safe. 137 (2015) 40-49.

[16] H.B. Liu, C. Jiang, X.Y. Jia, X.Y. Long, Z. Zhang, F. J. Guan, A new uncertainty propagation method for problems with parameterized probability-boxes, Reliab. Eng. Syst. Safe. 172(2018) 64-73.

[17] B. Echard, N. Gayton, M. Lemaire, N. Relun. A combined importance sampling and kriging reliability method for small failure probabilities with time-demanding numerical models, Reliab. Eng. Syst. Safe. 111(2013) 232-240

[18] P. Wei, F. Liu, C. Tang, Reliability and reliability-based importance analysis of structural systems using multiple response Gaussian process model, Reliab. Eng. Syst. Safe. 175(2018) 183-195.

[19] R. Schöbi, B. Sudret, Uncertainty propagation of p-boxes using sparse polynomial chaos expansions, J. Comput. Phys. 339(2017) 307-327.

[20] R. Schöbi, B. Sudret, Structural reliability analysis for p-boxes using multi-level meta-models, Probabilist. Eng. Mech. 48(2017) 27-38.

[21] X. Yang, Y. Liu, P. Ma, Structural reliability analysis under evidence theory using the active learning kriging model, Eng. Optimiz. 49 (2017) 1922-1938.

[22] S.K. Au, J.L. Beck, A new adaptive important sampling scheme, Struct. Saf. 21(1999) 135-158.

[23] G.I. Schuëller, H.J. Pradlwarter, P.S. Koutsourelakis, A critical appraisal of reliability estimation procedures for high dimensions, Probabilist. Eng. Mech. 19(2004) 463-473.

[24] S.K. Au, J.L. Beck, Estimation of small failure probabilities in high dimensions by subset simulation, Probabilist. Eng. Mech. 16(2001) 263-277.

[25] O. Ditlevsen, R.E. Melchers, H. Gluver, General multi-dimensional probability integration by directional simulation, Comput. Struct. 36(1990) 355-368.

[26] H. Zhang, H. Dai, M. Beer, W. Wang, Structural reliability analysis on the basis of small samples: an interval quasi-Monte Carlo method, Mech. Syst. Signal Process. 37 (2013) 137-151.

[27] P. Wei, Z. Lu, J. Song, Extended Monte Carlo simulation for parametric global sensitivity analysis and optimization, AIAA J. 52 (2014) 867-878.

[28] P. Wei, F. Liu, Z. Lu, Z. Wang, A probabilistic procedure for quantifying the relative importance of model inputs characterized by second-order probability models, Int. J. Approx. Reason. 98 (2018) 78-95

[29] J. Zhang, M. D. Shields, On the quantification and efficient propagation of imprecise probabilities resulting from small datasets, Mech. Syst. Signal Process. 98 (2018) 465-483.

[30] P. Wei, Z. Lu, J. Song, Regional and parametric sensitivity analysis of Sobol′ indices, Reliab. Eng. Syst. Safe 137(2015) 87-100.

[31] I.M. Sobol', S. Tarantola, D. Gatelli, S.S. Kucherenko, W. Mauntz, Estimating the approximation error when fixing unessential factors in global sensitivity analysis, Reliab. Eng. Syst. Safe 92 (2007) 957-960.

[32] P. Wang, Z.Z. Lu, K.C. Zhang, S.N. Xiao, Z.F. Yue, Copula-based decomposition approach for the derivative-based sensitivity of variance contributions with dependent variables, Reliab. Eng. Syst. Safe. 169(2018) 437-450.

[33] P.F. Wei, Z. Z. Lu, J. W. Song, Variable importance analysis: a comprehensive review. Reliab. Eng. Syst. Safe. 142(2015) 399-342

[34] G.Y. Li, S.W. Wang, High dimensional model representations generated from low dimensional data

samples. i. mp-cut-hdmr, J. Math. Chem. 30 (2001) 1-30.

[35] G.Y. Li, S.W. Wang, H. Rabitz, Practical approaches to construct RS-HDMR component functions. J. Phys. Chem. A, 106 (2002) 8721-8733.

[36] I. M. Sobol, S.S. Kucherenko, On global sensitivity analysis of quasi-monte Carlo algorithms, Monte Carlo Methods Appl. 11 (2005) 83-92.

[37] P. Wei, Z. Lu, J. Song, Variable importance analysis: a comprehensive review. Reliab. Eng. Syst. Safe., 142(2015), 399-432.

[38] S. F. Bi, M. Broggi, M. Beer, The role of the Bhattacharyya distance in stochastic model updating, Mech. Syst. Signal Process. 117(2019) 437-452